https://doi.org/10.5194/egusphere-2025-443
Preprint. Discussion started: 6 February 2025
© Author(s) 2025. CC BY 4.0 License.

Pathways of CH_4 formation and emission in the subsaline reed wetland of Lake Neusiedl

Pamela Alessandra Baur[1,2], Thiago Rodrigues-Oliveira[3], Karin Hager[3], Zhen-Hao Luo[3], Christa Schleper[2,3], and Stephan Glatzel[1,2]

[1]University of Vienna, Faculty of Earth Sciences, Geography and Astronomy, Department of Geography and Regional Research, Geoecology, Josef-Holaubek-Platz 2, 1090 Vienna, Austria.
[2]University of Vienna, Faculty of Life Sciences, Vienna Doctoral School of Ecology and Evolution (VDSEE), Djerassiplatz 1, 1030 Vienna, Austria.
[3]University of Vienna, Faculty of Life Sciences, Functional and Evolutionary Ecology, Djerassiplatz 1, 1030 Vienna, Austria.

Correspondence: Pamela Alessandra Baur (pamela.baur@univie.ac.at)

Abstract. Wetlands are a natural source of methane (CH_4) emissions and represent a substantial uncertainty in the global CH_4 budget. Furthermore, wetlands dominated by reed (*Phragmites australis*) have various CH_4 emission pathways, some of which are challenging to quantify (e.g., ebullition) or require additional research (e.g., plant-mediated transport) to reduce uncertainties and improve the accuracy of greenhouse gas balance models for wetlands. This field study investigates all CH_4 emission pathways (incl. diffusion) with various chamber types over four seasons and over the entire diel cycle (24 h) in the subsaline reed wetland of Lake Neusiedl in Austria. The pathways of CH_4 formation (methanogenesis) were examined in each season by determining $\delta^{13}C$ source signatures, and over the course of a year, by investigating specific microbial groups (methanogens, methanotrophs, and sulfate reducers) in the sediments. The highest CH_4 emissions were observed in summer, regardless of the emission pathway, with the highest emissions in all seasons occurring via the plant-mediated transport. Significant differences in CH_4 fluxes were observed between the plant-mediated transport and diffusion pathway in each season. However, a distinct diel cycle of CH_4 flux was exclusively observed via plant-mediated transport during summer. The source signatures $\delta^{13}C$-CH_4 exhibit seasonal variation, with the highest ^{13}C-depletion occurring in fall. Despite the different seasonal source signatures, the dominant methanogenic pathway remains acetoclastic throughout all seasons. Desiccation of the reed ecosystem resulted in a reduction in methanogenic microbial diversity in the sediments over the course of one year. Concurrently, the drought resulted in an increase and dominance of oxygen-tolerant *Methanomicrobiales*.

1 Introduction

Wetlands and their natural methane (CH_4) emissions (102–200 Tg CH_4 a^{-1}, 2008–2017) represent a significant source of uncertainty in the global CH_4 budget (Saunois et al., 2020). A more comprehensive understanding of the various emission pathways of wetlands is essential to reduce uncertainty and account for the high variability associated with the processes of CH_4 production, transformation, and consumption in various types of wetlands before it reaches the atmosphere (Rosentreter

https://doi.org/10.5194/egusphere-2025-443
Preprint. Discussion started: 6 February 2025
© Author(s) 2025. CC BY 4.0 License.

et al., 2021). This understanding is particularly crucial for vegetated wetlands, where plant-mediated CH_4 transport plays a significant role (Vroom et al., 2022).

In wetlands, methanogenesis predominately occurs in anoxic sediments and can be classified into three different methanogenic pathways based on the substrate utilized for microbial anaerobic CH_4 production (Conrad, 2020a): acetoclastic (acetate), hydrogenotrophic (H_2/CO_2), and methylotrophic (methyl compounds, e.g. methanol). The stable carbon isotope ratios of CH_4 and carbon dioxide (CO_2) can be employed to distinguish between biologic or thermogenic CH_4 sources, as well as to ascertain the dominant methanogenic pathway (Whiticar et al., 1986; Whiticar, 1999).

Wetlands dominated by reed (*Phragmites australis*) can be a highly dynamic mosaic of reed, water, and sediment patches that vary due to seasonal or environmental factors (Buchsteiner et al., 2023; Baur et al., 2024b). Consequently, these ecosystems exhibit different interfaces and emission pathways for CH_4 fluxes with the atmosphere. The plant-mediated transport of CH_4 via *P. australis* predominately occurs as pressurized convective gas flow (Armstrong and Armstrong, 1991; Brix et al., 2001), while molecular diffusion at the water-air and sediment-air interfaces represents another emission pathway. Additionally, ebullition as direct release of CH_4 bubbles from sediments, is another notable emission pathway. To date, only a few field studies have been conducted on all emission pathways of wetlands with reed. An experiment was conducted in a German fen lake with high water levels on three days in June 2013, which suggested that plant-mediated transport plays a more significant role as ebullition (van den Berg et al., 2020). Another study, conducted in a subtropical Australian wetland partially covered with *P. australis*, demonstrated that the plant-mediated transport had the highest CH_4 emissions in only one of the two field campaigns (Jeffrey et al., 2019). The few available studies on this subject and the inconclusive results illustrate the necessity for further field studies on reed wetlands. Such research should incorporate measurements of all emission pathways across all seasons. This would facilitate the determination of the precise contribution of plant-mediated CH_4 transport in comparison to the other emission pathways. It would also enhance the accuracy of greenhouse gas balance models for wetlands, as the contributions of the different emission pathways could be better represented (Vroom et al., 2022).

The diel (24 h) pattern of CH_4 emissions from aquatic macrophytes such as *P. australis* is highly influenced by the mode of gas transport and emission pathway (Chanton et al., 2002) and depends on the growth stage of the plant (Kim et al., 1998). In wetlands with reed, the diel variations in CH_4 emissions exhibited a wide range (2- to 5-fold) during the summer months (June–August/September), with the lowest emission occurring at night (Kim et al., 1998; van den Berg et al., 2016; Sanders-DeMott et al., 2022). However, the studies revealed discrepancies in the timing of the diel peak of CH_4 emissions during summer. Some studies have observed that this peak occurs around 12 o'clock (Kim et al., 1998; Sanders-DeMott et al., 2022; Zhang et al., 2016; van den Berg et al., 2016; Jeffrey et al., 2019), while others have reported that it occurs in the afternoon (Baur et al., 2024b; Philipp et al., 2017). Moreover, in a wetland with reed that is subject to drought, the diel variation of the total ecosystem CH_4 emissions is less pronounced and exhibits a different diel pattern with two peaks, which is likely due to CH_4 oxidation (Baur et al., 2024b). However, these studies have often focused on the total CH_4 emissions of the ecosystem, regardless of the emission pathways, or only on the summer season. However, there is a paucity of research examining diel patterns of each available emission pathway during all seasons, particularly in subsaline reed wetlands.

https://doi.org/10.5194/egusphere-2025-443
Preprint. Discussion started: 6 February 2025
© Author(s) 2025. CC BY 4.0 License.

An example of a reed-rich wetland environment that is subject to drought is Lake Neusiedl in Austria (Baur et al., 2024b). The lake is subsaline (Hammer, 1986), rich in sulfate (250–1250 mg SO_4^{2-} L^{-1} in 2021, Baur et al. (2024a)), and of international importance as UNESCO World Heritage site, Ramsar site, and transnational national park 'Neusiedler See – Seewinkel & Fertő – Hanság'. The reed ecosystem covers 181 km^2 (Csaplovics, 2019) of the lake and is the largest connected reed area in Europe after the Danube delta.

The presence of specific microbial groups, including methanogens, sulfate reducers, and methanotrophs, within sediments can provide valuable insights into the reed ecosystem. Indeed, these microbial communities serve as indicators of environmental conditions, offering a window into the complex interactions, processes, and methanogenic pathways occurring within the sediments and beyond (Hilderbrand et al., 2020; Soman et al., 2024; Zhang et al., 2020). Sulfate-reducing bacteria convert SO_4^{2-} into less oxidized sulfur compounds, such as hydrogen sulfide (H_2S), to derive energy, a process driven by the availability of hydrogen (H_2) (Muyzer and Stams, 2008) and is often coupled to CH_4 oxidation (Valentine, 2002; Hoehler et al., 1994). Methanogens are well known for being the producers of CH_4 in various environments, with wetlands constituting the main natural sources of this gas on the planet (Wang et al., 1996). Methanogenesis is particularly relevant when considering that it is the final step of organic matter degradation in anoxic ecosystems (Schlesinger and Bernhardt, 2013). It is therefore of particular interest to examine wetlands with reed, where the CH_4 production or oxidation in the rhizosphere can be highly influenced by the gas transport (oxygen (O_2), CO_2 and CH_4) (Brix et al., 2001; Armstrong and Armstrong, 1990) and root exudates of reed (van den Berg et al., 2016). Furthermore, the presence of soda salts and sulfate represents a specific set of environmental conditions for subsaline reed ecosystems of inland waters (Baur et al., 2024a), underscoring the need for microbial investigation.

The objective of this study is to address the following research questions in the subsaline reed wetland of Lake Neusiedl: **(a)** Does the CH_4 flux show a distinct diel cycle in different emission pathways or seasons? **(b)** Which emission pathway dominates the diel CH_4 fluxes in which season, and what is its contribution? **(c)** To what extent can the microbial community or $\delta^{13}C$ source signatures explain the CH_4 formation or emission dynamics?

In order to answer these questions, we carried out various chamber measurements during all seasons, determined isotopic source signatures, analyzed sediment properties, and investigated the microbial community in the sediments.

2 Material and Methods

2.1 Study site

Lake Neusiedl (Fertő) on the Austrian–Hungarian border with an area of 315 km^2 (Wolfram and Herzig, 2013) is the western-most steppe lake in Europe with no natural outflow, but with an artificial outlet, which is closed since mid-2015 due to low water levels (Baur et al., 2024b). The lake is very shallow, with declining annual maximum water levels from 1.66 m (2018) to 1.33 m (2022) due to drought (Baur et al., 2024b). The major salt of the subsaline lake is sodium bicarbonate (Wolfram and Herzig, 2013). More than half of the lake is covered by a reed ecosystem dominated by *Phragmites australis*. Due to drought,

https://doi.org/10.5194/egusphere-2025-443
Preprint. Discussion started: 6 February 2025
© Author(s) 2025. CC BY 4.0 License.

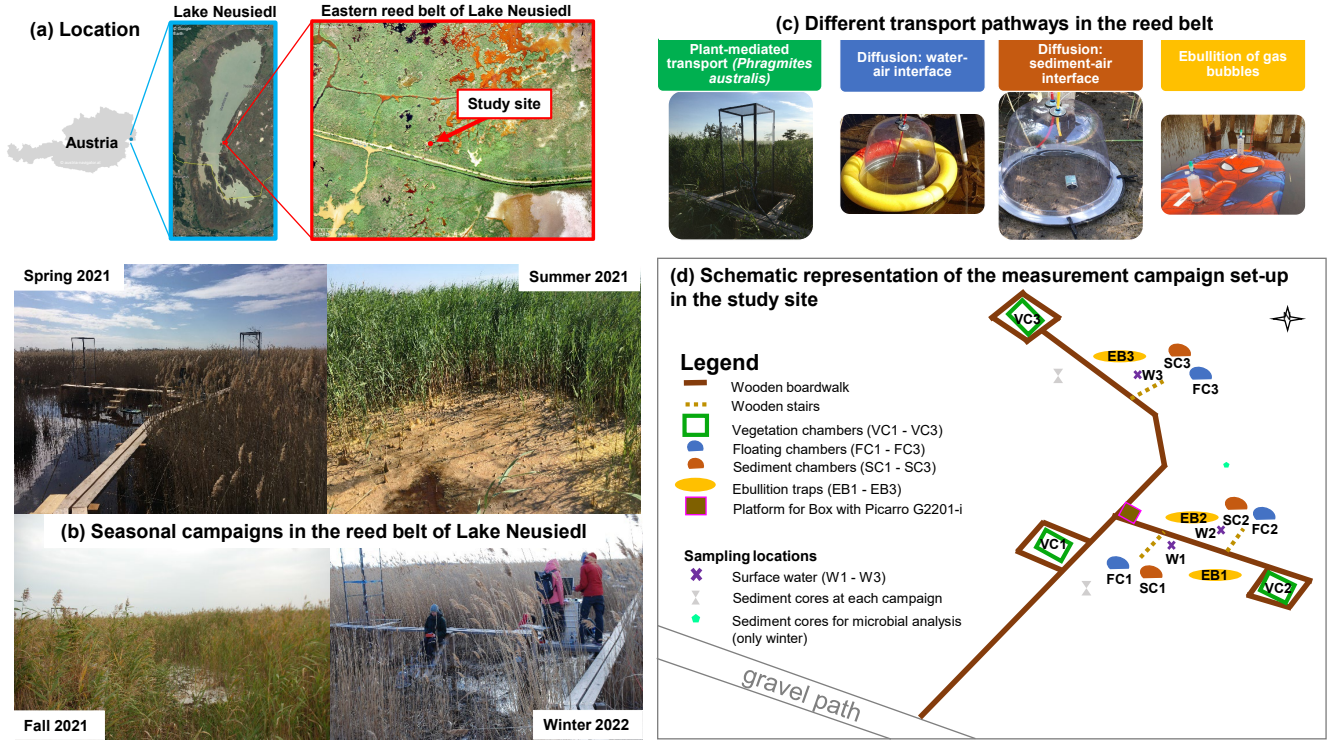

Figure 1. The study site is **(a)** located in the eastern reed belt of Lake Neusiedl in Austria and was used for **(b)** intensive 24 h measurement campaigns in each season. The different emission pathways of the CH_4 fluxes in the reed belt were measured with four chamber types illustrated in **(c)**. The setup of the measurement campaigns is shown in a schematic representation in **(d)**.

the mosaic of the reed belt has exhibited a notable increase in reed and open sediment areas, but also a corresponding loss of water areas during the years 2021 and 2022 (Buchsteiner et al., 2023; Baur et al., 2024b).

The study site (Lat: 47.7693°, Long: 16.7576°) is situated in the eastern reed belt of Lake Neusiedl near the Biological Station Lake Neusiedl (Illmitz, Austria) and in the nature zone of the national park (see Fig. 1a). In order to prevent any disturbance during the measurements, a boardwalk was constructed in the reed belt in December 2020. The site has a mean annual air temperature of 11.3°C and an annual precipitation of 500.2 mm (1993–2022) (Baur et al., 2024b).

2.2 Measurement setup

We conducted intensive 24 h measurement campaigns in each season (spring, summer, fall, winter; see Fig. 1b) to investigate the diel variability of CH_4 fluxes for each available emission pathway and their seasonal variability in the reed belt. As the reed belt is a dynamic mosaic of reed, water, and open sediment area that vary according to season and condition, the reed belt has different exchange interfaces with the atmosphere. For that reason, chamber and ebullition trap measurements were conducted for each emission pathway with the objective of investigating their respective contributions and dominance within the reed belt:

https://doi.org/10.5194/egusphere-2025-443
Preprint. Discussion started: 6 February 2025
© Author(s) 2025. CC BY 4.0 License.

Table 1. The mean ± standard deviation of meteorological, water, and reed properties of the reed belt at our study site during the seasonal 24 h measurement campaigns (T_{air} = air temperature, rH = relative humidity, LAI = leaf area index, T_{water} = water temperature, WL = water level, EC = electrical conductivity, DO = dissolved oxygen, ORP = oxygen–reduction potential, Chl-a = Chlorophyll-a, SO_4^{2-} = sulfate, and TOC = total organic carbon concentration of the surface water, if water was present).

Season	DOY	Year	T_{air} [°C]	rH [%]	LAI	T_{water} [°C]	WL [cm]	pH_{water}	EC_{water} [mS cm^{-1}]	DO_{water} [%]	ORP_{water} [mV]	Chl-a_{water} [μg L^{-1}]	$Sulfate_{water}$ [mg L^{-1}]	TOC_{water} [mg L^{-1}]
spring	88 & 89	2021	14.3 ± 3.1	57.8 ± 19.0	0.7 ± 0.4	14.9 ± 2.8	20 ± 3	8.40 ± 0.04	3.26 ± 0.02	78.7 ± 10.8	139.8 ± 40.5	1.4 ± 3.1	576.7 ± 12.6	48.6 ± 2.8
summer	179 & 180	2021	26.8 ± 6.5	64.1 ± 19.8	2.5 ± 1.1	27.5 ± 5.8	4 ± 3	8.98 ± 0.04	6.92 ± 0.40	69.8 ± 78.1	−172.6 ± 105.2	34 ± 30	1379.0 ± 109.1	133.3 ± 16.7
fall	271 & 272	2021	15.9 ± 4.7	86.3 ± 12.5	1.4 ± 0.6	-	0	-	-	-	-	-	-	-
winter	53 & 54	2022	5.4 ± 2.8	71.9 ± 17.3	-	7.1 ± 3.7	4 ± 1	8.89 ± 0.08	5.93 ± 0.57	98.6 ± 19.1	−18.7 ± 106.4	37 ± 43	1040.1 ± 154.7	124.1 ± 15.2

plant-mediated transport of *P. australis*, diffusion at the water–air and sediment–air interfaces, and ebullition (see Fig. 1c). The spring campaign took place on 29 and 30 March 2021, the summer campaign on 28 and 29 June 2021, the fall campaign on 28 and 29 September 2021, and the winter campaign on 22 and 23 February 2022. In addition to seasonal fluctuations, there was a sharp decline in water levels in the study area, particularly in 2021 (and 2022; see Baur et al. (2024b)), indicating that the reed belt had experienced a prolonged dry period following the summer campaign. The meteorological conditions, water, and reed properties of the studied reed belt during the campaigns are pictured in Fig. 1b and summarized in Table 1. During the study period, the surface water of the reed belt showed water levels ranging from 0 to 23 cm (see Table 1). If water was present, pH values ranged from 8.4 to 9 and electrical conductivity from 3.3 to 7 mS cm^{-1}.

The measurement intervals in a 24 h measurement campaign were every 3 h for each chamber type and every 6 h for gas bubbles in the ebullition traps. There were 3 replicates of each chamber type and 9 replicates of ebullition traps (funnels) spatially distributed around the constructed boardwalk at the study site (see Fig. 1d).

Sediment cores were sampled in each campaign and analyzed in the laboratory for chemical and physical properties (see Section 2.3.1 for details). In order to determine the microbial status in the sediments and its changes over time, two sediment cores were taken before the first and after the last measurement campaign (one year apart) and are described in Section 2.3.2.

2.2.1 Pathways divided by different chamber measurements and ebullition traps

Different measurement types were used to capture the different emission pathways of CH_4 fluxes in the reed belt individually: plant-mediated transport of *P. australis* with vegetation chambers (VC), diffusion at the water–air interface with floating chambers (FC), diffusion at the sediment–air interface with sediment chambers (SC), and ebullition with ebullition traps (EB) (see Fig. 1c). The setup of the campaigns with the location of the chambers and the sampling points is schematically represented in Fig. 1d. The dry mole fraction of CH_4 and the stable carbon isotope ratios (δ^{13}C-CH_4 and δ^{13}C-CO_2) of the chamber air were measured directly in the field with an isotopic gas analyzer (G2201-i, Picarro Inc., Santa Clara, USA) using cavity ring-down spectroscopy (CRDS; highly sensitive laser absorption technology). All isotopic ratios measured in this study are expressed in ‰ relative to Vienna Pee Dee Belemnite (VPDB). Before each campaign, the instrument was calibrated using two certified stable isotope standard gases, which are described in Baur et al. (2024a). The δ^{13}C-CH_4 values of the collected

https://doi.org/10.5194/egusphere-2025-443
Preprint. Discussion started: 6 February 2025
© Author(s) 2025. CC BY 4.0 License.

gas from EB were measured with the same instrument in the lab shortly after each campaign (for further details, please refer to Baur et al. (2024a)).

The stable carbon isotope ratio δ^{13}C-CH_4 can be used to differentiate the biological and geological sources of CH_4 emissions (Whiticar et al., 1986) and, in combination with δ^{13}C-CO_2, to examine the mechanisms of CH_4 production and oxidation (Whiticar, 1999). The isotopic signature of the CH_4 source in each season was determined using the Keeling plot approach (Keeling, 1958; Pataki et al., 2003) and is the intercept of the linear regression between the reverse values of dry mole CH_4 fraction and the values of δ^{13}C-CH_4. The CO_2 source was determined in a similar manner, albeit with CO_2 values.

VCs were used to capture the plant-mediated transport of *P. australis*. For each VC, a steel frame (2.99 m × 0.78 m × 0.78 m) was welded with a ground frame (0.2 m × 0.78 m × 0.78 m), which was anchored permanently at the study site since early March 2021 and inserted at least 7 cm into the ground. At the beginning of each campaign, every VC was covered with transparent acryl glass plates (3 walls and 1 lid), which were all surrounded with highly strong magnetic stripes. A mobile acryl glass plate equipped with an inlet tube plug-in connector, an outlet tube plug-in connector, and a power cable was used to close the chamber during measurements. Each VC had three fans at three different heights to ensure good ventilation inside the chamber.

FCs were used to capture the transport of molecular diffusion at the water–atmosphere interface and are described in detail in Baur et al. (2024a). SCs were used to capture the molecular diffusion transport at the sediment–atmosphere interface. The SC top was made of transparent PVC in the form of a growing bell with a diameter of 30 cm and a hard plate with sealing rubber on the base. The bottom frame was an aluminum ring surrounded by a sealing rubber, which was inserted to the sediments 2–3 weeks in advance of each campaign. The upper chamber and the bottom frame were fixed and held together with at least 5 clamps during each measurement.

During measurements, SC, VC, and FC were directly connected to the Picarro instrument (and a pump) through two 6 mm outer diameter polyurethane tubes (Festo GmbH, Esslingen, Germany), one as inlet and another as outlet, which circulated the air between the closed chamber and the instrument. The closing time for FC and SC was 5 min each, the VC closing time was 10 min due to the larger chamber volume.

EBs were used to capture the ebullition pathway of gas bubbles from supersaturated sediments and are described in detail in Baur et al. (2024a). This study of Baur et al. (2024a) examined the ebullition pathway continuously over a more extended period (from March to July 2021) at the same lake and not solely within the reed belt.

During the spring campaign, there were no open sediment areas at the study site due to higher water levels within the reed belt, which precluded the possibility of performing SC measurements. During the course of the year, due to the sharp drop in water levels not only in the open lake area of Lake Neusiedl, but also in the reed belt (Baur, 2024), EB and FC measurements were not possible in fall, as there was no water level above the surface. Furthermore, it was not feasible to conduct EB measurements during the winter season, as the exceedingly low water levels precluded the installation of the inverted funnels, which would have entailed contact with and disturbance of the sediments.

https://doi.org/10.5194/egusphere-2025-443
Preprint. Discussion started: 6 February 2025
© Author(s) 2025. CC BY 4.0 License.

2.2.2 Flux calculation

For the calculation of the fluxes of the chamber measurements (FC, SC, and VC), the initial 25 % of the chamber closure time (death band) was removed from the linear regression fit of the temporal change of the dry mole fractions of CH_4 to exclude potential artifacts due to chamber closing (Hoffmann et al., 2017). Ebullition (sudden exponential increase in the dry mole fraction) during chamber measurements was excluded for the calculation of diffusive fluxes. Due to the presence of a highly agile sediment layer (soft, waterlogged), ebullition was at times triggered due to the closure of the SC during the summer campaign. However, given the aim of measuring diffusion rates at the soil–air interface with the SC, unfortunately it was necessary to exclude a substantial proportion of SC measurement data. The equations utilized to estimate chamber fluxes and ebullition rates are thoroughly delineated in Baur et al. (2024a). Only flux data from FC, SC, and VC were utilized that exhibited a coefficient of determination R^2 of at least 0.6 for the linear regression of the temporal change of the dry mole fractions of CH_4, or in instances where the CH_4 flux was minimal (near zero), i.e. between -0.01 and 0.01 mg CH_4 m^{-2} h^{-1} and the R^2 was at least 0.6 for the temporal change of the dry mole fraction of CO_2. In total, 213 chamber CH_4 fluxes were used, with a mean R^2 of 0.9. Additionally, 72 ebullition rates were calculated across two season campaigns (spring and summer), of which 26 exhibited ebullition rates exceeding zero.

2.2.3 Environmental variables

Each SC and FC was equipped inside with an air temperature and a light sensor (HOBO Pendant Temperature/Light 8K Data Logger, Onset Computer Corporation, Bourne, USA) with a measurement time interval of 30 sec. Each VC was equipped inside with an air temperature and relative humidity sensor (HOBO U23 Pro v2 Temperature/Relative Humidity Data Logger, Onset Computer Corporation, Bourne, USA) with a measurement time interval of 10 sec. Under each floating board with three ebullition traps, a water temperature sensor (HOBO Pendant Temperature/Light 8K Data Logger, Onset Computer Corporation, Bourne, USA) was fixed with a measurement time interval of 30 min due to the smaller data memory. Additionally, ambient air temperature, water vapor pressure deficit (VPD), incoming shortwave radiation (SW_{in}), and sediment temperature (in 5 cm depth) were measured nearby (50 m distance) at an eddy covariance tower (detailed description in Baur et al. (2024b) and published data in Baur (2024)).

2.3 Sediment sampling and analysis

In each campaign, at least two sediment cores were sampled with polycarbonate push core tubes (diameter 7 cm, length 60 cm). Each sediment core was divided according to its two visibly distinct layers for physical and chemical analysis. Fresh samples of each layer were sieved with a 2 mm sieve to remove large rhizomes, large roots or snail shells.

Additionally, two sediment cores for microbial analysis were sampled in the reed belt always in winter before the first (11 February 2021) and after the last campaign (23 February 2022) using push core tubes, which were sealed with Parafilm after sampling. The sediment cores were divided into 2 cm depth sections in an anaerobic tent filled with nitrogen (N_2), individually packed, sealed, and stored at 4°C in a refrigerator until laboratory analysis. The microbial analysis was carried

https://doi.org/10.5194/egusphere-2025-443
Preprint. Discussion started: 6 February 2025
© Author(s) 2025. CC BY 4.0 License.

out in four specific depth sections of each sediment core, two of which belong to the same layer: 0–2 cm, 4–6 cm, 20–22 cm, 24–26 cm.

2.3.1 Physical and chemical sediment characterization

The gravimetric water content (WC) of the sediments was determined by completely drying the accurately weighed wet sample in the freeze dryer (Lio 5P, Kambic d.o.o., Semic, Slovenia) until constant dry weight. WC was calculated according to Gardener (1986).

The completely dry sediment samples were finely ground (pulverized) and homogenized with a mixer mill (MM400, RETSCH GmbH, Haan, Germany). A multiphase carbon analyzer (RC612, LECO Europe B.V., AG Geleen, Netherlands) was used to determine the organic (TOC, ≤ 450°C), inorganic (TIC, > 450°C & ≤ 1000°C), and total carbon content (TC, sum of TOC and TIC) of the samples (in percent per dry weight) via temperature dependent CO_2 measurement (dry combustion method).

For the analysis of sulfate, ammonium, nitrate, nitrite, and orthophosphate in the sediments, sediment extracts were prepared from 4 g field moist sediment samples and 30 mL extraction solution (0.01 M $CaCl_2 \cdot 2H_2O$ for sulfate; ultra-pure distilled water for the other parameters). The sediments were extracted on a horizontal shaker at 300 rpm for 60 min at room temperature to obtain optimal suspension of the slurry. The extracts were filtered using 0.45 μm nylon syringe filters. The concentrations of the extracts were determined by turbidity or colorimetry using a uv-vis spectrometer (Infinite 200 Pro NanoQuant, Tecan Group Ltd., Männedorf, Switzerland). The specific methods are described in detail in Baur et al. (2024a).

For the pH and electrical conductivity (EC), the sediment samples were air dried at 40°C until mass stability. The samples were then incubated with ultra-pure distilled water overnight (ratio 1:10 w/v), shaken for 1 h in an overhead shaker and left standing for 30 min prior to measurements of pH (pHmeters pH 7110 and pH 720, WTW GmbH, Weilheim, Germany) and EC (Cond 7110, Xylem Analytics Germany GmbH, Weilheim, Germany).

2.3.2 Microbial 16S rRNA gene amplification, sequencing and analysis

Each sediment depth section sample, weighing between 0.5 to 1.0 g, underwent DNA (deoxyribonucleic acid) extraction utilizing the DNeasy PowerSoil Pro Kit (Qiagen NV, Venlo, Netherlands), following the manufacturer's guidelines. Subsequently, DNA concentration was determined using a Qubit 2.0 Fluorometer (Invitrogen, Carlsbad, USA) equipped with the dsDNA HS kit. For amplification of prokaryotic 16S rRNA genes, we employed PCR (polymerase chain reaction) with the primer pair 515f (5'- GTG CCA GCM GCC GCG GTA A) and 806r (5'- GGA CTA CHV GGG TWT CTA AT), as detailed previously (Caporaso et al., 2011). The PCR products were then barcoded and sequenced at the Vienna BioCenter Core Facilities (VBCF) on the Illumina Miseq platform (300 PE). The initial raw reads underwent preprocessing using cutadapt (Martin, 2011) to eliminate primer sequences, followed by sequence analysis via the QIIME2 pipeline (Bolyen et al., 2019). In summary, the data was denoised and filtered for low-quality reads and chimeras using the DADA2 algorithm. Subsequently, sequences exhibiting 100 % identity were clustered into amplicon sequence variants (ASVs). Taxonomic classification of these ASVs was conducted utilizing the SILVA database (release 138) in conjunction with the 'q2-feature-classifier' plugin (Bokulich et al., 2018).

https://doi.org/10.5194/egusphere-2025-443
Preprint. Discussion started: 6 February 2025
© Author(s) 2025. CC BY 4.0 License.

2.4 Data and statistical analysis

Most data and statistical analysis were performed in R, version 4.2.2 (R Core Team, 2022), using the following R packages for data processing, manipulation and visualization: *data.table, ggplot2, ggpubr, scales, hms* (Müller, 2023; Barrett et al., 2024; Kassambara, 2023a; Wickham, 2016; Wickham et al., 2023).

The two-sided Dunn's post-hoc test was applied using the R package *rstatix* (Kassambara, 2023b) to statistically assess which emission pathway or season had significant differences in median CH_4 fluxes compared to the others and in sediment properties between the two sediment layers ($p < 0.05$, Adjustment Holm). Linear ordinary least squares regression using the R package *lmodel2* (Legendre, 2018) was used to determine the $\delta^{13}C$ source signatures in Keeling plots.

Potential interactions between the methanogenic archaea and other microbes were investigated by employing SparCC (Sparse Correlations for Composition data) network (Friedman and Alm, 2012) analysis at the ASVs level. Only those with > 10 reads and detected in > 20 % of the samples were used for network construction to prevent false associations caused by low abundant ASVs. 1000 bootstraps were used and those with $p < 0.05$ were retained. The positive relationships (correlation coefficient > 0) were summarized at the class level. Only the top 10 groups with highest number of potential interactions with methanogenic archaea were shown, with network visualization being conducted in Cytoscape (Shannon et al., 2003).

3 Results

3.1 Seasonal and diel differences in CH_4 emissions of a subsaline reed wetland

Plant-mediated transport exhibited significantly elevated CH_4 emissions compared to emissions through diffusion or ebullition pathways throughout all seasons, as illustrated in Table 2. Regardless of the emission pathway, the highest median CH_4 emission rate and fluctuation range occurred during the summer campaign. The highest CH_4 emission of 18.56 mg CH_4 m^{-2} h^{-1} was observed via plant-mediated transport at 15 o'clock during the summer campaign. In summer, the median CH_4 emissions at the two diffusion interfaces (water–air and sediment–air) and the ebullition pathway did not show significant differences. However, in winter, the water–air interface exhibited a median CH_4 flux of 0.05 mg CH_4 m^{-2} h^{-1}, which was more than 10-fold and significantly higher than that observed at the sediment–air interface. Almost all emission pathways exhibited a significantly different median CH_4 flux between the seasons. Only at the sediment–air interface, the median flux did not differ significantly between fall and winter. The ebullition pathway exhibited the most pronounced fluctuations in CH_4 emissions across the two seasons in which EB measurements were possible, and demonstrated the lowest emission rate in spring. In spring, bubbles were trapped in only 3 % of the EB measurements, while in summer it happened in 69 %. The measurement of all pathways was not possible in all seasons due to variations in water levels and the dryness of the reed belt (see Fig. 1).

https://doi.org/10.5194/egusphere-2025-443
Preprint. Discussion started: 6 February 2025
© Author(s) 2025. CC BY 4.0 License.

Table 2. Differences in CH_4 fluxes for each emission pathway (plant-mediated, water–air interface, sediment–air interface, ebullition) and season are represented by their median ± standard deviation; significant differences ($p < 0.05$ with Holm's adjustment, Dunn's test) between the pathways in each season are indicated by different superscript letters, between the seasons in each pathway by different superscript symbols or between daytime and nighttime in each pathway and season by different superscript numbers; the number of quality checked measurement data is provided in brackets; due to the water level or dryness of the reed belt, not every pathway could be measured in each season; nighttime when incoming shortwave radiation was < 10 W m^{-2}.

		CH_4 flux [mg CH_4 m^{-2} h^{-1}]			
Time period	**Pathways**	**Spring 2021**	**Summer 2021**	**Fall 2021**	**Winter 2022**
diel (24 h)	plant-mediated	$1.36 \pm 0.23^{a,+}(24)$	$4.59 \pm 3.61^{d,*}(24)$	$0.35 \pm 0.30^{f,\otimes}(24)$	$0.12 \pm 0.06^{h,\wedge}(24)$
	water-air	$0.11 \pm 0.07^{b,\cap}(23)$	$1.12 \pm 0.51^{e,\pi}(16)$	-	$0.05 \pm 0.06^{i,\cup}(23)$
	sediment-air	-	$1.21 \pm 0.52^{e,\backslash}(08)$	$0.002 \pm 0.01^{g,\oplus}(24)$	$0.004 \pm 0.09^{k,\oplus}(23)$
	ebullition	$0.000 \pm 1.00^{c,\Omega}(36)$	$1.35 \pm 3.69^{e,\Phi}(36)$	-	-
daytime	plant-mediated	$1.54 \pm 0.23^{a,+,1}(13)$	$6.37 \pm 3.90^{d,*,2}(15)$	$0.52 \pm 0.38^{f,+\wedge,4}(10)$	$0.11 \pm 0.05^{h,\wedge,5}(9)$
	water-air	$0.14 \pm 0.08^{b,\cap,6}(12)$	$1.07 \pm 0.42^{e,\pi,8}(12)$	-	$0.06 \pm 0.02^{hk,\cup,9}(9)$
	sediment-air	-	$1.21 \pm 0.48^{e,\backslash,10}(06)$	$0.001 \pm 0.01^{g,\oplus,11}(11)$	$0.006 \pm 0.10^{k,\otimes,12}(11)$
	ebullition	$0.000 \pm 1.41^{c,\Omega,13}(18)$	$1.28 \pm 3.77^{e,\Phi,14}(27)$	-	-
nighttime	plant-mediated	$1.23 \pm 0.22^{a,+,1}(11)$	$3.19 \pm 1.60^{d,+,3}(09)$	$0.29 \pm 0.21^{f,\wedge,4}(14)$	$0.12 \pm 0.06^{h,\wedge,5}(15)$
	water-air	$0.09 \pm 0.04^{b,\pi\cup,7}(11)$	$1.59 \pm 0.60^{d,\pi,8}(04)$	-	$0.03 \pm 0.08^{hk,\cup,9}(14)$
	sediment-air	-	$1.48 \pm 0.84^{d,\oplus,10}(02)$	$0.002 \pm 0.01^{g,\oplus,11}(13)$	$0.001 \pm 0.08^{k,\oplus,12}(12)$
	ebullition	$0.000 \pm 0.00^{c,\Omega,13}(18)$	$2.31 \pm 3.59^{d,\Phi,14}(09)$	-	-

Only plant-mediated transport showed a clear visible diel cycle of CH_4 fluxes in summer with the highest emission rates during daytime and on average a peak in the late afternoon (see Fig. 2). In contrast, the diffusion pathways showed only some small diel variations, but no distinct diel cycle. However, we were able to detect a decrease in diffusive CH_4 fluxes at the water–air interface around midday in summer. In spring and fall, only plant-mediated transport displayed some diel variations of CH_4 fluxes, but not the diffusion pathways. Significant differences in the median CH_4 flux between daytime and nighttime (SW_{in} < 10 W m^{-2}) were identified for only two emission pathways, occurring in one season each: water–air in spring and plant-mediated in summer (see Table 2). Given that the ebullition trap measurements were consistently obtained over a 6 h period, we have not plotted a fitted line of diel variations, as the precise timing of bubble release from the sediments remains uncertain. Instead, the observed CH_4 ebullition rate was placed in the middle of the 6 h bubble collecting time in Fig. 2. During the spring campaign, only one ebullition rate of 5.98 mg CH_4 m^{-2} h^{-1} could be observed during daytime. In contrast, during the summer campaign, ebullition occurred at nighttime and during daytime, with the highest rate of 17.03 mg CH_4 m^{-2} h^{-1}.

https://doi.org/10.5194/egusphere-2025-443
Preprint. Discussion started: 6 February 2025
© Author(s) 2025. CC BY 4.0 License.

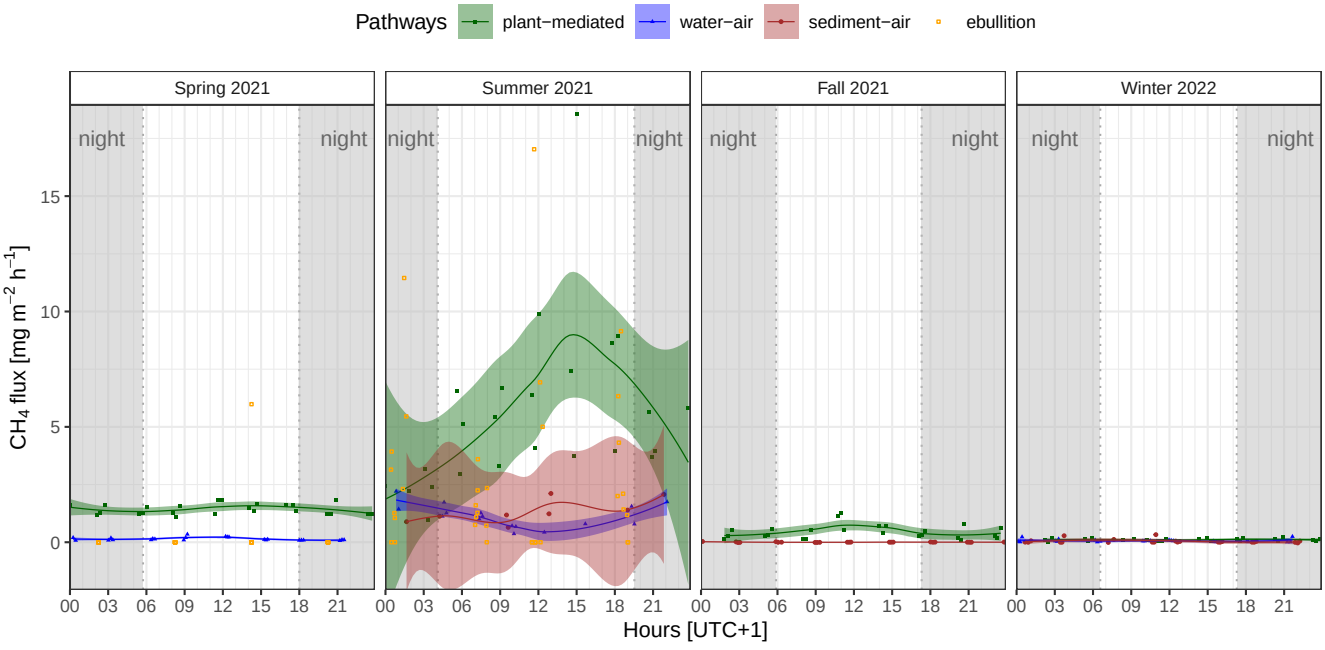

Figure 2. Diel variability of the CH_4 fluxes for each season and emission pathway (plant-mediated, water–air interface, sediment–air interface, ebullition); the fitted lines showing the local polynomial regressions (loess) with the 95 % confidence interval; due to the water level or dryness of the reed belt, not every pathway was present or could be measured in each season; nighttime when incoming shortwave radiation was < 10 W m^{-2} (gray shading).

3.2 Seasonal δ^{13}C source signatures of a subsaline reed wetland

The Keeling plots' source signatures δ^{13}C-CH_4 differ between seasons and are most ^{13}C-depleted in fall (-73.6 ± 2.4 ‰ VPDB; see Fig. 3a). The Keeling plots' source signatures δ^{13}C-CO_2 differ between seasons and are most ^{13}C-depleted in winter (-30 ± 1.6 ‰ VPDB; see Fig. 3b). The methanogenic characterization after Whiticar et al. (1986) indicates the dominance of acetoclastic methanogenesis in the reed belt of Lake Neusiedl regardless of the seasons (see Fig. 3c). However, the values of the source signatures including the standard error of the winter campaign are already partially within the range of CH_4 oxidation in this representation. For this subsaline reed wetland, the mean of the seasonal isotopic source signatures are -63.6 ± 2.7 ‰ VPDB for CH_4 and -28.1 ± 1.2 ‰ VPDB for CO_2.

The δ^{13}C-CH_4 values of the collected ebullition gases were -54.2 ‰ VPDB (N = 1) in the spring campaign and -59.9 ± 1.9 ‰ VPDB (N = 25) in the summer campaign. In fall and winter, no ebullition trap measurements were possible due to the dryness of the reed belt.

https://doi.org/10.5194/egusphere-2025-443
Preprint. Discussion started: 6 February 2025
© Author(s) 2025. CC BY 4.0 License.

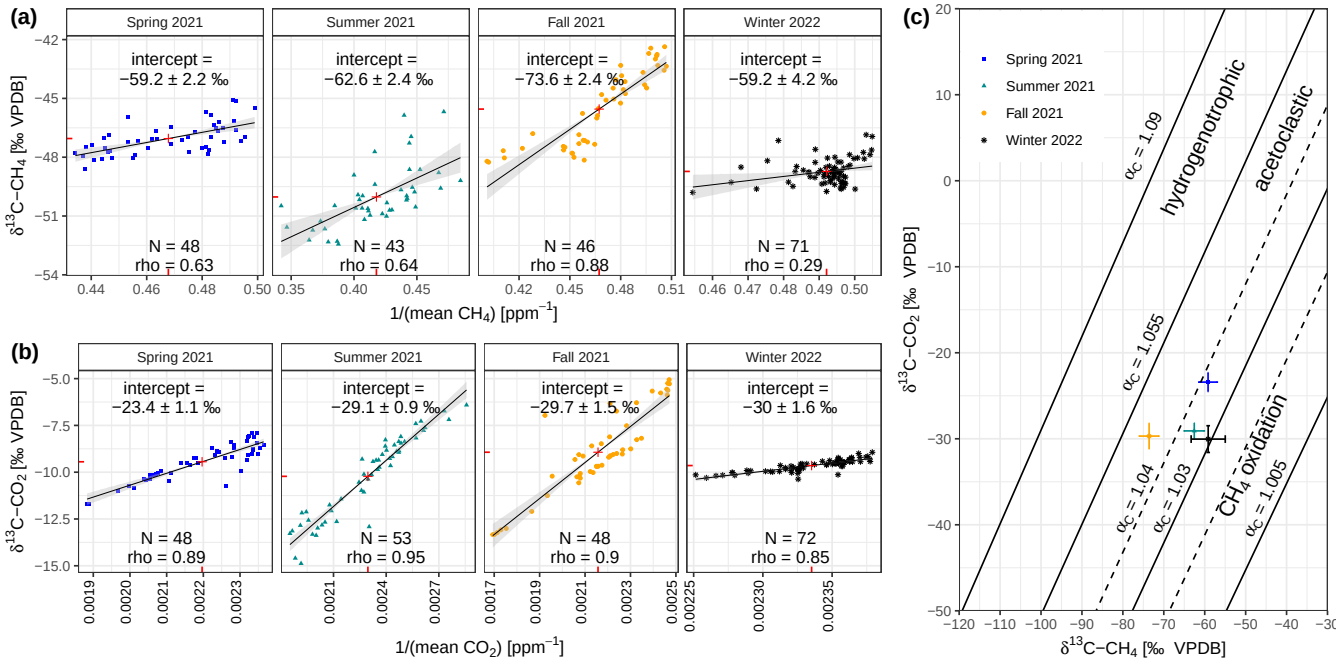

Figure 3. Keeling plots to determine the seasonal source signatures **(a)** δ^{13}C-CH_4 and **(b)** δ^{13}C-CO_2 of the reed belt as the y axis intercepts (shown as number in ‰ VPDB) of the fitted ordinary least square linear regression lines (black) with 95 % confidence interval (shaded light gray) and their centroids (red cross), and **(c)** the methanogenic characterization according to Whiticar et al. (1986) using the source signature pairs of δ^{13}C-CH_4 and δ^{13}C-CO_2 and their standard errors.

3.3 Sediment properties of the reed belt

The sediments of the reed belt of Lake Neusiedl had two clear distinguishable layers with significant differences in most physical and chemical parameters (see Fig. 4 and A2). The upper layer (L1) was very wet (mean ± standard deviation of gravimetric WC: 82.3 ± 6.7 mass-%, see Fig. 4b), brown, peaty (mean TOC: 18.2 ± 9.6 mass-%, see Fig. 4a), and with a mean thickness of 9.7 ± 3.8 cm. The lower layer (L2) was gray, sandy, and low in organic carbon (mean TOC: 0.8 ± 0.6 mass-%). In spring, L1 was a fluffy layer, had the highest water level above it (20 ± 3 cm), and had occasionally a maximum thickness of 19 cm. However, there were no significant differences in L1 thickness between seasons. In contrast, the TOC and TIC values of L1 in particular differed between the seasons (see Fig. 4a and A2a). The mean TIC decreased from spring to winter, while the mean TOC increased during the same period, except for the mean value of the summer season. The SO_4^{2-} concentration in the sediments showed the same seasonal pattern as the TOC values (see Fig. 4a and c). L1 showed the highest concentration of NH_4^+ in summer and the highest concentration of NO_2^- in fall (see Fig. A2d and f). The upper sediment layer exhibited, on average, a significantly higher EC value and a significantly lower pH value compared to the lower layer (see Fig. A2g and h).

https://doi.org/10.5194/egusphere-2025-443
Preprint. Discussion started: 6 February 2025
© Author(s) 2025. CC BY 4.0 License.

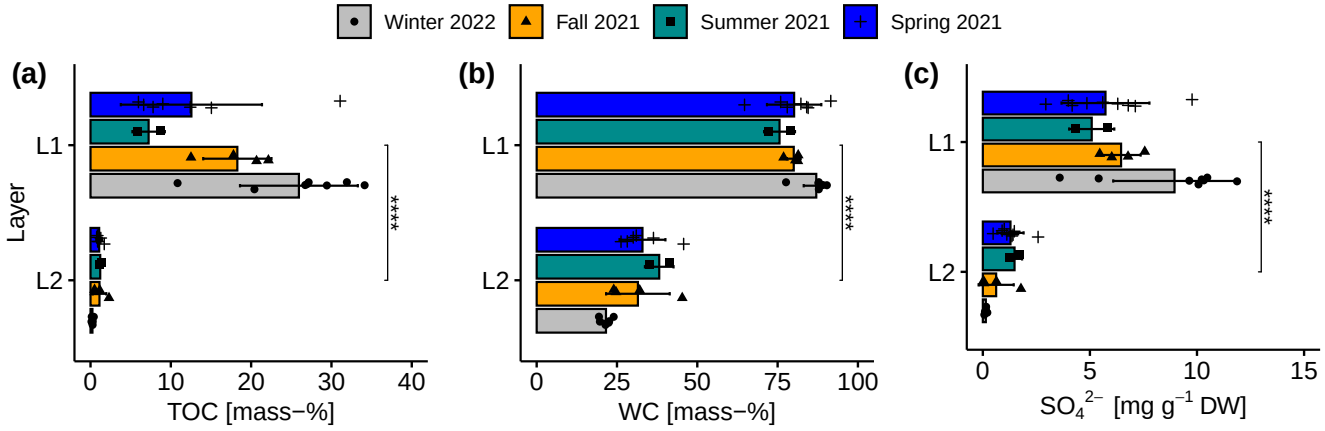

Figure 4. Seasonal and layer specific differences of **(a)** total organic carbon content (TOC), **(b)** gravimetric water content (WC), and **(c)** sulfate (SO_4^{2-}) concentration in the upper (L1) and lower layer (L2) of sediments in the reed belt of Lake Neusiedl. Very significant differences (****, $p < 0.0001$ with Holm's adjustment, Dunn's test) in the parameters between the two layers in the sediments independent of the season.

3.4 Change in the microbial community in the sediments within one year

Considering the findings regarding CH_4 fluxes throughout 2021, and acknowledging the central role the microorganisms play in CH_4 emission dynamics, our study investigated the microbial community composition within sediments from Lake Neusiedl at two different sampling dates: one in winter 2021 and another a year later in winter 2022. We conducted our analysis across various depths in two sediment cores each winter, employing prokaryotic 16S rRNA gene amplicon sequencing. It is worth pointing out that there was a marked decrease in total DNA yield in samples from the lower layers in comparison to those from the upper layers, with a decrease of almost 1000-fold in 2021 and almost 32-fold in 2022 (see Table A1). Due to the significance of sulfate-reducing bacteria, methanogens, and methanotrophs in carbon cycling within anaerobic sediment environments (Jones, 1985; Conrad, 2007; Muyzer and Stams, 2008), we specifically targeted these three groups for further investigation (see Fig. 5). The amplicon sequencing quality of core II at the depth of 4–6 cm from the 2022 sampling was insufficient for its inclusion in further analyses.

Examination of the distribution pattern of methanogens (see Fig. 5a) reveals a noticeable trend: their relative abundance is higher in the lower depths (20–22 cm and 24–26 cm) samples compared to the upper layer in both years, although this difference is less pronounced in the 2021 sampling. When comparing their diversity across the two years, various observations emerge. First, in 2022, their relative abundance was substantially higher, reaching up to 12 % compared to a maximum of around 2 % in 2021. Second, the composition of methanogenic communities differed substantially. In 2021, sediments exhibited a broader array of detected methanogenic groups, encompassing orders such as *Methanobacteriales*, *Methanosarcinales*, *Methanococcales*, *Methanomicrobiales*, and *Methanomassiliicoccales*. Conversely, in 2022, the methanogenic community displayed greater homogeneity, predominantly dominated by organisms from the order *Methanomicrobiales*.

https://doi.org/10.5194/egusphere-2025-443
Preprint. Discussion started: 6 February 2025
© Author(s) 2025. CC BY 4.0 License.

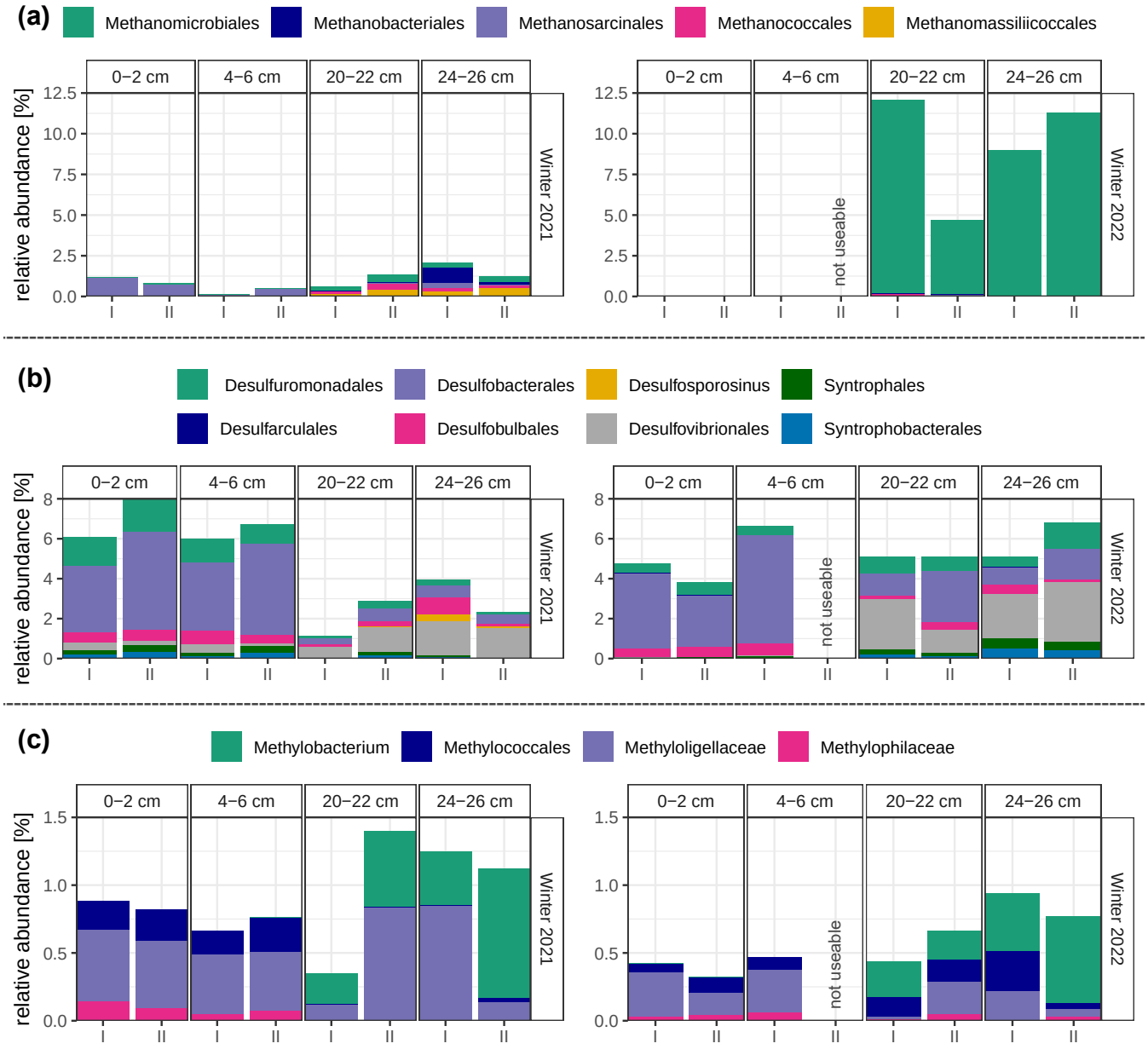

Figure 5. Relative abundance of **(a)** methanogens, **(b)** sulfate-reducing bacteria, and **(c)** methanotrophs in four depth sections of the two sediment cores (I and II) in winter 2021 and 2022. The two sediment sections, 0–2 cm and 4–6 cm, are part of the top organic layer (L1) of the sediment, while the sections 20–22 cm and 24–26 cm are located in the lower sandy layer (L2). Due to the insufficient amplicon sequencing quality of core II at the depth of 4–6 cm from the 2022 sampling, the sample was not used for further analyses.

https://doi.org/10.5194/egusphere-2025-443
Preprint. Discussion started: 6 February 2025
© Author(s) 2025. CC BY 4.0 License.

The relative abundances of sulfate-reducing bacteria (see Fig. 5b) display a distinct trend in the year 2021. There is a marked discrepancy between the upper (0–2 cm and 4–6 cm) and the lower layer (20–22 cm and 24–26 cm). In the upper layer, the relative abundance of sulfate-reducing bacteria is higher, reaching levels of up to around 8 %, in contrast to the deeper layer where it reaches numbers of around 4 %. This difference in abundance is accompanied by a visible diversity pattern. The upper layer predominantly hosts taxa such as *Desulfobacterales*, *Desulfuromonadales*, and *Desulfobulbales*. While these groups persist in the lower layer, there is a shift towards an increased prevalence of organisms belonging to the order *Desulfovibrionales*, eventually becoming the most abundant sulfate-reducing bacterial group in the 24–26 cm depth. The sediments sampled in 2022 present a different pattern, with comparable sums of relative abundances of sulfate reducers across different depths in 2022 in contrast to 2021. However, the dominant taxa are similar to those observed in the previous year, where the same groups are also prevalent in the upper layer, and *Desulfovibrionales* becomes more abundant as depth increases.

Analysis of methanotroph distribution reveals similar patterns across samplings from both 2021 and 2022 (see Fig. 5c). In both years, a clear distinction is observed between the upper and lower layer, with *Methylobacterium* being detected exclusively in depths $\geq$ 20 cm, while *Methyloligellaceae* and *Methylococcales* dominate the upper layer (0–2 cm and 4–6 cm). However, there is an overall lower relative abundance of methanotrophs across all depths in 2022 compared to 2021, with maximum values of approximately 0.9 % compared to 1.4 %.

A network interface of significant non-random relationships between the different hydrogenotrophic methanogenic groups and other microbes in the Lake Neusiedl sediment community was constructed (see Fig. 6). We obtained 1,398 nodes (ASVs) and 132,305 edges, and after clustering and filtering, a co-occurrence network with 153 nodes and 325 edges were generated. In the network, the groups that displayed the highest number of relationships with methanogens included *Aminicenantales*, *Anaerolineales*, *Bacteroidales*, *Burkholderiales*, *Desulfatiglandales*, *Desulfobacterales*, *Pseudomonadales*, *Sedimentisphaerales*, and *Woesearchaeales*.

https://doi.org/10.5194/egusphere-2025-443
Preprint. Discussion started: 6 February 2025
© Author(s) 2025. CC BY 4.0 License.

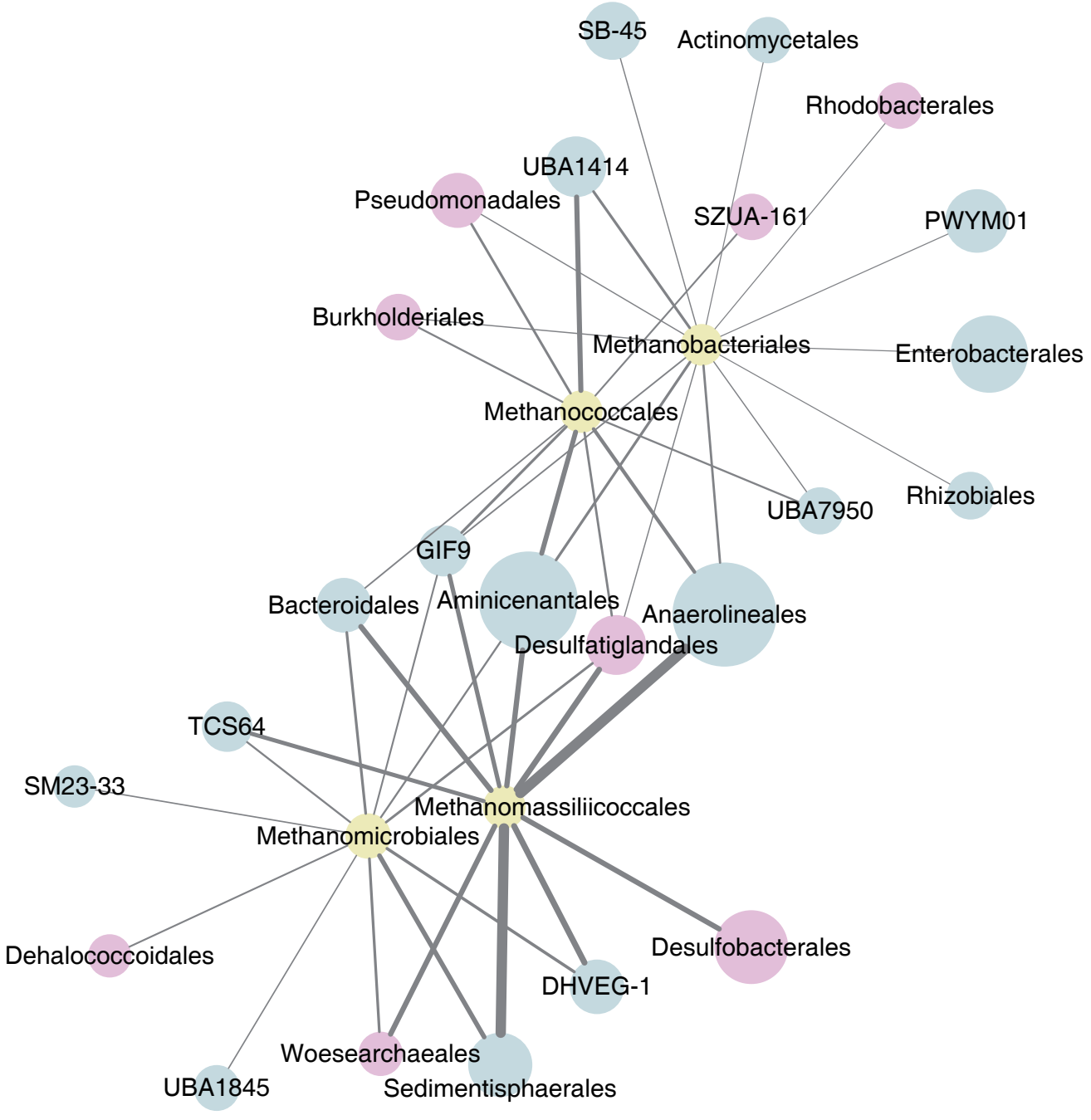

Figure 6. Co-occurrence network ($p < 0.05$) of hydrogenotrophic methanogens (yellow) with other microbes, with groups containing organisms with potential for acetate oxidation highlighted (pink). Only the top 10 microbes (blue) with links to methanogens were included. The size of each node is proportional to the relative abundance of the group and the thickness of each line is proportional to the number of links between the nodes.

https://doi.org/10.5194/egusphere-2025-443
Preprint. Discussion started: 6 February 2025
© Author(s) 2025. CC BY 4.0 License.

4 Discussion

4.1 Seasonal and diel differences in CH_4 fluxes for each emission pathway in a subsaline reed wetland

This is one of the first studies to date to investigate all possible CH_4 emission pathways in a wetland with reed over the entire diel cycle (24 h) and in all seasons individually. In the studied subsaline reed wetland, plant-mediated transport was identified as the most significant emission pathway for CH_4, irrespective of the season.

The highest seasonal median plant-mediated CH_4 flux (summer) at our studied wetland with reed is approximately half that of the average plant fluxes from studies of littoral zones in lakes or wetlands (8.3 mg CH_4 m^{-2} h^{-1}), as reported by Bastviken et al. (2011). Moreover, our observed flux is 4 to 10 times lower than that reported in studies of other wetlands with reed (van den Berg et al., 2020; Duan et al., 2006) and twice as high as the flux observed in a subtropical *Phragmites* wetland subjected to drought (Jeffrey et al., 2019). One possible explanation for this discrepancy is the influence of lower water levels, given that Lake Neusiedl was experiencing drought (Baur et al., 2024b). A second possible explanation is that the subsaline reed ecosystem exhibited lower CH_4 production rates than the fen (van den Berg et al., 2020), which may be attributed to the coexistence and competition of sulfate reducers and methanogens.

The plant-mediated CH_4 fluxes at our site were consistently higher than diffusive CH_4 fluxes at the water–air and sediment–air interfaces, also in the non-growing season. One potential explanation is the chimney effect, which has been observed in the context of standing dead or non-intact reed culm between the sediment and the atmosphere (van den Berg et al., 2020; Brix, 1989). An additional potential explanation is Venturi-induced flow, as observed by Armstrong et al. (1992) in *P. australis*. This phenomenon is wind-induced and is likely to occur during the winter months when humidity-induced convection is absent.

In reed ecosystems, a clear diel cycle of CH_4 fluxes is only observed when pressurized flow is present, as opposed to diffusion. Pressurized flow is contingent upon the presence of living and intact reed culm (van den Berg et al., 2020; Vroom et al., 2022). Accordingly, at our site, a distinct diel cycle of CH_4 fluxes was discerned solely in summer and in instances of plant-mediated transport. However, when the reed ecosystem is considered as a whole and without partitioning in emission pathways, the reed belt exhibited a diel cycle with two peaks (with a slightly higher peak in the afternoon) during the summer months of 2021 (Baur et al., 2024b). This phenomenon is likely caused by CH_4 oxidation during daytime due to the low or absent water levels above the sediments (Baur et al., 2024b). The higher water level would also account for van den Berg et al. (2020)'s observation of a distinct diel cycle of CH_4 fluxes in June, both at the ecosystem level and in plant-mediated transport.

It can be reasonably assumed that the pressurized flow at our site is primarily driven by humidity and temperature. These findings are corroborated by observations that the plant-mediated CH_4 fluxes of *P. australis* exhibited a peak in the diel cycle in summer in the late afternoon, as did sediment temperature (in 5 cm depth) and VPD (see Fig. A1). In addition to light, these drivers were also identified by Vroom et al. (2022). In a reed wetland in an arid region of China, the diel cycle was explained by light-induced convection flow and the peak often occurred in the afternoon, coinciding with the time of the highest sediment temperature (Duan et al., 2006). In contrast, in a fen with reed, the peak of diel CH_4 fluxes were around midday (van den Berg et al., 2020), which could indicate the higher influence of light intensity and the lack of influence of soil temperature due to the high water levels. Another study conducted in the Hungarian part of Lake Neusiedl on 30 June 1993 revealed a daily maximum

https://doi.org/10.5194/egusphere-2025-443
Preprint. Discussion started: 6 February 2025
© Author(s) 2025. CC BY 4.0 License.

of pressure and flow in the efflux reed culms in the afternoon (Brix et al., 1996), indicating a potential contribution of old reed stubbles to the afternoon peak of diel CH_4 fluxes. At our site, there are enough standing dead and broken reed culm in summer to potentially exert an influence.

The ebullition rates at our site are, on average, lower than the plant-mediated CH_4 emissions, with a notable increase observed in summer compared to spring. The median summer ebullition rate of 1.35 mg CH_4 m^{-2} h^{-1} is comparable to the average ebullition rates observed in a subtropical wetland (partially covered with reed) across two seasons (Jeffrey et al., 2019). However, at our study site, the release of ebullition was found to be highly sporadic and less frequent in spring. Consequently, ebullition measurements require the use of longer periods than 24 h outside of summer. Baur et al. (2024a) employed a sampling frequency of one week at Lake Neusiedl to more effectively capture the natural sporadic release of ebullition gases from April to July 2021.

4.2 Seasonal methanogenic characterization with δ^{13}C source signatures of a subsaline reed wetland

The present study demonstrated that a subsaline reed wetland exhibits seasonal variability in the source signatures δ^{13}C-CH_4 and δ^{13}C-CO_2. The most ^{13}C-depleted δ^{13}C-CH_4 source signature of -73.6 ‰ VPDB was observed in fall and may be attributed to the greater availability of substrates (acetate) at this time of year. In contrast, the most ^{13}C-enriched δ^{13}C-CH_4 source signatures were observed in spring and winter (-59.2 ‰ VPDB) and are likely due to reduced substrate availability (Sriskantharajah et al., 2012). Fisher et al. (2017) previously assumed seasonal variability in the isotopic source signatures of diel measurements in a Finish fen, with the most ^{13}C-depleted δ^{13}C-CH_4 in fall (October). However, their study did not cover all seasons.

Our summer δ^{13}C-CH_4 source signature of -62.6 ± 2.4 ‰ VPDB indicates a greater ^{13}C-enrichment compared to the summer source signature of boreal wetlands, which has been determined to be -70.9 ± 1.2 ‰ (Fisher et al., 2017). Whereas, the seasonal mean δ^{13}C-CH_4 source signature of our site (-63.6 ‰ VPDB) is slightly more ^{13}C-depleted than the ones from tropical reed wetlands with -62.7 ‰ (Hong Kong) or -59.6 ‰ (Zambia) (France et al., 2022). Fisher et al. (2017) elucidated the discrepancies observed in wetlands situated in more southern latitudes as a consequence of enhanced CH_4 oxidation in warmer wetlands, which exhibit thicker oxic layers, and due to variations in methanogenic communities. In our case, CH_4 oxidation was likely further facilitated by drought, resulting in a source signature comparable to that observed in tropical wetlands with reed.

This study corroborates the utility of Keeling plots derived from data of diel chamber measurements as a means of identifying source signatures of wetlands (Fisher et al., 2017). In summer, the δ^{13}C-CH_4 source signature shows a high correspondence with the δ^{13}C-CH_4 values of the collected ebullition gases. The source signatures illustrate, according to the methanogenic characterization plot of Whiticar et al. (1986), the predominance of acetoclastic methanogenesis across all seasons in the reed ecosystem under study. Until now, the dominance of acetoclastic methanogenesis at this site has only been confirmed during the April to July period by analyzing the ebullition gas (Baur et al., 2024a). However, the winter source signature indicates an influence of CH_4 oxidation due to the desiccation of the reed belt.

https://doi.org/10.5194/egusphere-2025-443
Preprint. Discussion started: 6 February 2025
© Author(s) 2025. CC BY 4.0 License.

4.3 Change of the sediment microbial community in a subsaline reed ecosystem within one year

The variations observed in the methanogenic community of Lake Neusiedl between the two sampling years include differences in both relative abundance and diversity. Despite their higher relative abundance of methanogens, the overall microbial biomass in the deeper layer was consistently low across both years, as evidenced by the little DNA yield from these samples (see Table A1). *Methanomicrobiales*, an order detected in both 2021 and 2022, exhibited particularly high abundance in the latter year. Members of this group utilize H_2, CO_2, formate, and alcohols for methanogenesis (Garcia et al., 2006). *Methanococcales* and *Methanobacteriales*, also detected in 2021, encompass primarily hydrogenotrophic organisms (Bonin and Boone, 2006; Whitman and Jeanthon, 2006).

Notably, our campaign results indicate CH_4 production due to acetoclastic methanogenesis across all seasons. This process is exclusively carried out by representatives of *Methanosarcinales* (Stams et al., 2019), and while present in both years, these organisms were more prevalent in 2021 with lower levels detected in 2022. While it is worth pointing out that 16S rRNA gene relative abundance does not necessarily correlate to activity, these methanogens could be playing an important role in the CH_4 levels detected. Furthermore, syntrophic acetoclastic methanogenesis is known to occur, especially in environments less conducive to *Methanosarcinales* (Hattori, 2008). In this context, acetate is oxidized by organisms such as syntrophic acetate oxidizing bacteria, Woesearchaea, some sulfate-reducing bacteria, among others, and the resulting H_2 could be used for hydrogenotrophic methanogenesis (Lee and Zinder, 1988; Spormann and Thauer, 1988; Galushko and Kuever, 2019; Castelle et al., 2021; Huang et al., 2021). Interestingly, the co-occurrence network analysis (see Fig. 6) of sediment samples from Lake Neusiedl shows possible syntrophic interactions between hydrogenotrophic methanogenic orders and examples of such groups (highlighted in pink), indicating that syntrophic acetoclastic methanogenesis might be further contributing to the observed results. Moreover, the consistent detection of methanotrophs across all layer in both years could have affected the CH_4 levels measured in the present study, as these organisms have been shown to potentially consume a substantial amount of upward CH_4 fluxes in sediments (Valentine and Reeburgh, 2000).

The different levels of O_2 tolerance and sensitivity of methanogens may explain the differences in occurrences between the two sediment layers. Furthermore, the change in methanogenic taxa between the two winters (2021 and 2022) can be attributed to the drying of the study site from mid-July 2021, which resulted in the formation of cracks where the sediments could come into increased contact with O_2. First, we observed a (near) absence of methanogens in the upper layer in winter 2022 after desiccation, which could indicate that oxic conditions were dominant in this layer. Secondly, only the O_2-tolerant methanogens, such as for example *Methanosarcina subterranea* and *Methanosarcina siciliae* belonging to *Methanosarcinales* group (Conrad, 2020b; Lyu and Lu, 2018; Horne and Lessner, 2013; Angel et al., 2011), were present in the upper layer in winter 2021, when the study site was flooded. This indicates that the O_2 delivery to the rhizosphere may have occurred through the aerenchyma of *P. australis* (Armstrong et al., 1992), thereby influencing the O_2 content in this sediment layer, as standing water was above the sediments in winter 2021. Third, after desiccation, a marked increase and dominance of *Methanomicrobiales*, which are O_2-tolerant methanogens (Conrad, 2020b; Lyu and Lu, 2018), was observed in the lower layer. Fourth, the lower layer prior to desiccation exhibited a high diversity of methanogens, including those belonging to the O_2 sensitive *Methanobacteriales* and

https://doi.org/10.5194/egusphere-2025-443
Preprint. Discussion started: 6 February 2025
© Author(s) 2025. CC BY 4.0 License.

Methanococcales (Conrad, 2020b; Lyu and Lu, 2018). However, these were absent after desiccation. These observed changes are inconsistent with the findings of Conrad (2020b), who was able to find methanogenic population dynamics after desiccation, but not with O_2 sensitivity as the exclusive criterion.

Considering that the sulfate reduction zone typically occurs closer to the surface compared to the methanogenesis zone (Jørgensen and Kasten, 2006), the observed higher relative abundance of sulfate-reducing bacteria in the upper layer and methanogens in the lower layer is not surprising. Furthermore, the increased detection of *Desulfovibrionales* with depth could be a consequence of a decrease in organic matter in the deeper layer (see Fig. 4a), as members of this group have been shown to thrive in oligotrophic environments (Sass et al., 1998; Bade et al., 2000; Wörner and Pester, 2019). The detection of sulfate-reducing bacteria across both years draws attention due to their metabolic features in aquatic sediments. Acetate and H_2 serve as substrates for both sulfate reduction and methanogenesis (Schink, 1997; Conrad, 1999). Sulfate-reducing bacteria hold a thermodynamic advantage over methanogens, as they can utilize acetate and H_2 at lower concentrations, potentially outcompeting methanogens for substrate uptake. This process channels electron flow towards CO_2 production rather than CH_4 (Lovley et al., 1982; King, 1984; Lovley and Goodwin, 1988). However, it is worth noting that these organisms and processes can co-occur, as observed in environments such as the sulfate-methane transition zone, and could be coupled in ways that influence substrate production and consumption rates (Egger et al., 2016; Sela-Adler et al., 2017). Thus, it is possible that similar interactions occur in Lake Neusiedl. The higher relative abundance of sulfate reducers in the upper layer, followed by a decrease in their levels in the lower layer coinciding with an increase in methanogen relative abundance, suggests a putative competition scenario where methanogens may have been outcompeted for resources when sulfate reducers were more prevalent. Moreover, the consistent detection of methanotrophs across all layers in both years could have affected the CH_4 levels measured in the present study, as these organisms have been shown to potentially consume a substantial amount of upward CH_4 fluxes in sediments (Valentine and Reeburgh, 2000).

5 Conclusions

This study shows that in a wetland with reed, a distinct diel cycle of CH_4 fluxes occurs only in the emission pathway of plant-mediated transport and in the summer season. The plant-mediated transport pathway demonstrated the highest CH_4 emissions not only in summer, but also during other seasons. The distinct differences in the two sediment layers, namely in terms of carbon and water content, are also reflected in the variations observed in the microbial communities. The desiccation process resulted in a reduction in the methanogenic microbial diversity in the sediments over the course of a year. The findings of this study can be extended to other wetlands with reed vegetation, particularly those situated in similar subsaline or brackish conditions, or to other wetlands experiencing drought conditions. However, additional research is required to determine whether the methanogenic diversity will recover following an increase in water levels in reed wetlands.

https://doi.org/10.5194/egusphere-2025-443
Preprint. Discussion started: 6 February 2025
© Author(s) 2025. CC BY 4.0 License.

Appendix A: Reed belt of Lake Neusiedl

A1 Diel and seasonal differences in biometeorological parameters

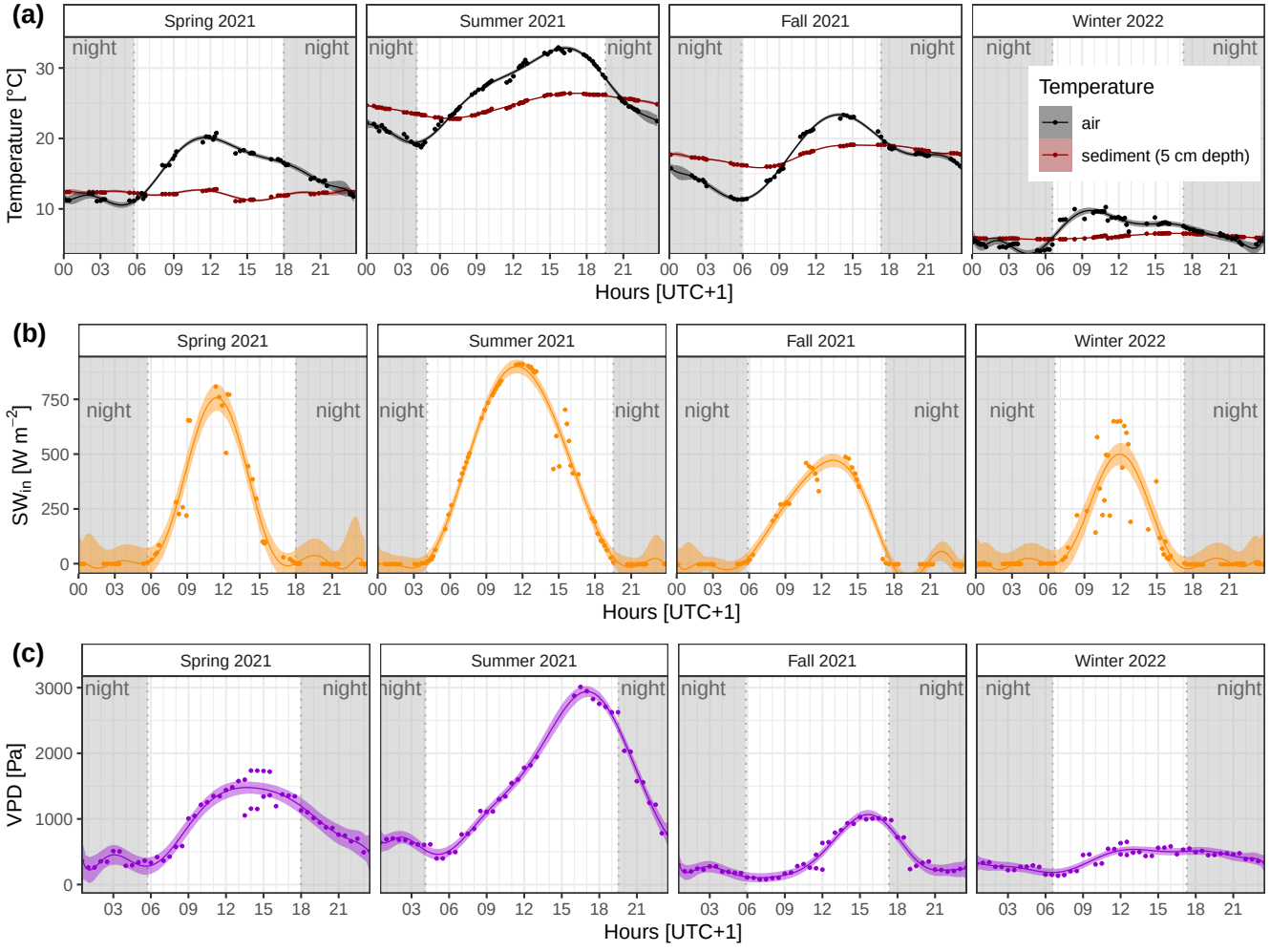

Figure A1. Diel and seasonal differences in **(a)** ambient air and sediment temperature, **(b)** incoming shortwave radiation (SW_{in}), and **(c)** water vapor pressure deficit (VPD) in the reed belt of Lake Neusiedl (data source: Baur (2024)); the fitted lines showing the decic polynomial regressions with the 95 % confidence interval; nighttime when SW_{in} was < 10 W m^{-2} (gray shading).

https://doi.org/10.5194/egusphere-2025-443
Preprint. Discussion started: 6 February 2025
© Author(s) 2025. CC BY 4.0 License.

A2 Seasonal and layer specific differences in sediment properties

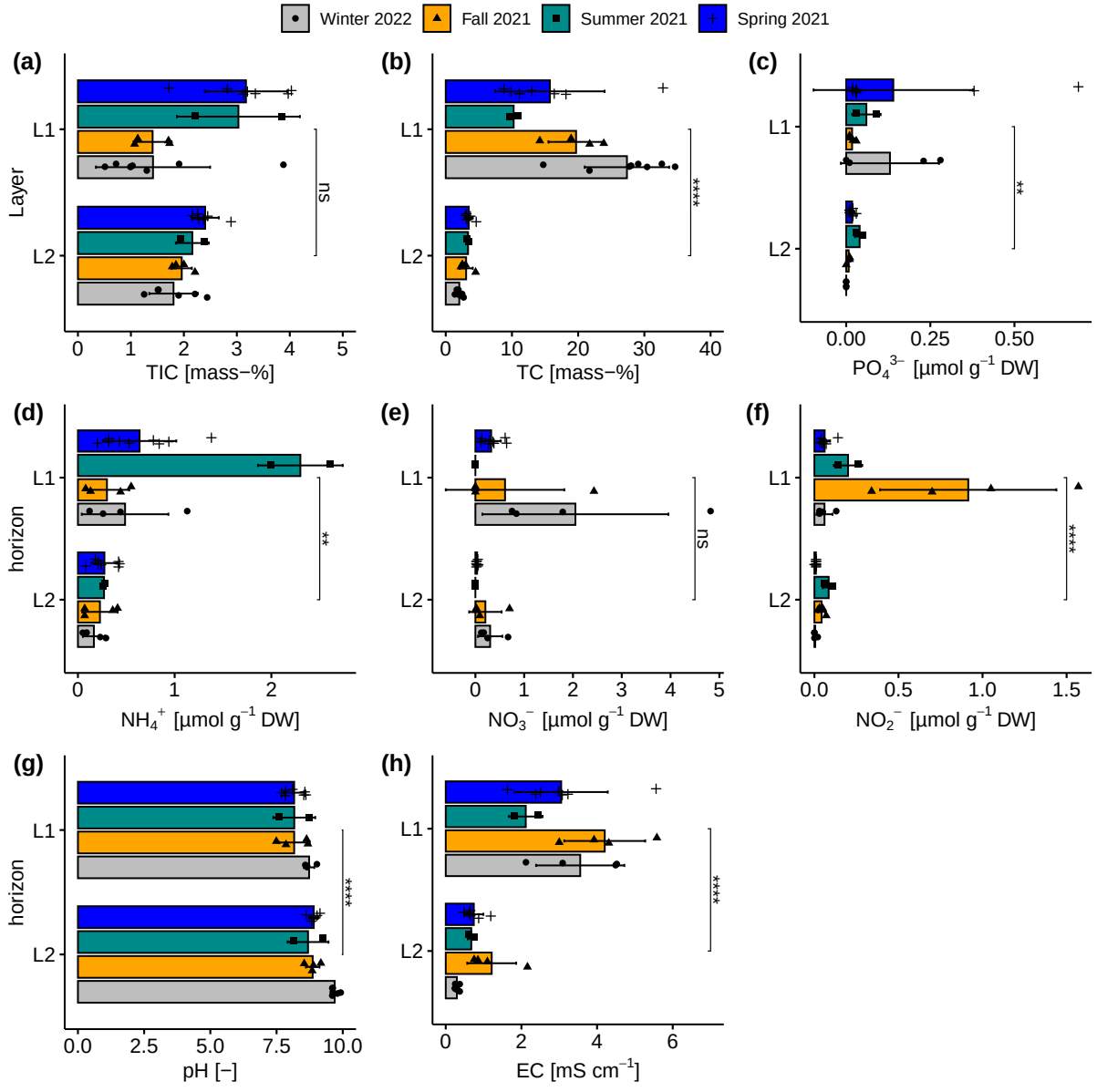

Figure A2. Seasonal and layer specific differences of **(a)** total inorganic carbon content (TIC), **(b)** total carbon content (TC), **(c)** phosphate (PO_4^{3-}), **(d)** ammonium (NH_4^+), **(e)** nitrate (NO_3^-), **(f)** nitrite (NO_2^-) concentration, **(g)** pH, and **(h)** electrical conductivity (EC) in the upper (L1) and lower layer (L2) of sediments in the reed belt of Lake Neusiedl. Non-significant (ns, $p > 0.05$ with Holm's adjustment, Dunn's test), significant (**, $p < 0.01$) or very significant differences (****, $p < 0.0001$) in the parameters between the two layers in the sediments independent of the season.

https://doi.org/10.5194/egusphere-2025-443
Preprint. Discussion started: 6 February 2025
© Author(s) 2025. CC BY 4.0 License.

A3 Inter-annual differences in properties and microbial characteristics of sediments

Table A1. DNA yield, total number of microbial classes, gravimetric water content (WC), and total organic carbon content (TOC) in four depth section of the sediment cores I and II from the reed belt of Lake Neusiedl in winter 2021 and 2022. The two sediment sections, 0–2 cm and 4–6 cm, are part of the upper layer (L1) of the sediment, while the sections 20–22 cm and 24–26 cm are located in the lower layer (L2).

Season	**Core**	**Depth section** [cm]	**DNA yield** [μg g^{-1} DW]	**Number of classes**	**TOC** [mass-%]	**WC** [mass-%]	**pH**	**EC** [mS cm^{-1}]
Winter 2021	**I**	0–2	41.172	143	33.2	89.1	8.36	3.35
		4–6	39.549	146	35.1	89.6		
		20–22	0.033	112	0.5	24.8	9.13	0.34
		24–26	0.042	124	0.8	31.0	8.76	0.88
	II	0–2	43.571	162	31.5	90.8	8.12	2.25
		4–6	42.747	166	30.9	89.6	8.33	2.56
		20–22	0.037	127	0.3	26.3	9.10	0.35
		24–26	0.001	84	0.2	21.4	9.34	0.35
Winter 2022	**I**	0–2	8.058	141	29.4	87.8	8.65	4.49
		4–6	9.889	134	31.9	87.8		
		20–22	0.628	108	0.4	24.0	9.60	0.37
		24–26	0.300	117	0.3	21.4	9.59	0.32
	II	0–2	7.899	127	26.8	88.0	8.65	4.52
		4–6	7.844		26.7	89.1		
		20–22	0.558	158	0.1	19.4	9.62	0.25
		24–26	0.282	106	0.3	22.6	9.53	0.33

https://doi.org/10.5194/egusphere-2025-443
Preprint. Discussion started: 6 February 2025
© Author(s) 2025. CC BY 4.0 License.

Data availability. The sediment, isotope and flux data generated in this study will be made available in the Phaidra repository of the University of Vienna under https://doi.org/10.25365/phaidra.626. All 16S rRNA raw sequences data are available at the NCBI database under the project identifier PRJNA1182700.

Author contributions. PAB: conceptualization, data curation, formal analysis, investigation, methodology, project administration, software, validation, visualization, writing - original draft preparation, writing - review & editing; TRO: conceptualization, data curation, formal analysis, methodology, writing - original draft preparation, writing - review & editing; KH: data curation, formal analysis, methodology; ZHL: data curation, formal analysis, visualization, writing - review & editing; CS: funding acquisition, resources, supervision; SG: funding acquisition, resources, supervision, writing - review & editing.

Competing interests. The authors declare no conflict of interest.

Acknowledgements. We highly acknowledge the intensive field and lab support of the Geoecology team and others: Claudia Buchsteiner, Daniela Henry, Andreas Maier, Raphael Müller, Sebastian Echeverria, Camila Aguetoni Cambui, Katharina Fischer, Yujing Deng. We thank the team of Thomas Zechmeister from the Biological Station Lake Neusiedl (Illmitz, Austria) for their support in the construction of the boardwalk and water analyses in the lab. We also thank the national park 'Neusiedler See – Seewinkel' for access to the study area, the granting of permits and the friendly cooperation. We would like to thank the Burgenland Provincial Government for granting the permit ('Naturschutzbehördliche Ausnahmegenehmigung') for entering the national park nature zone and conducting research there.

Financial support. This research was funded in part by the Austrian Science Fund (FWF) [10.55776/Z437] and in part by ERC AdvGrant TACKLE (695192).

https://doi.org/10.5194/egusphere-2025-443
Preprint. Discussion started: 6 February 2025
© Author(s) 2025. CC BY 4.0 License.

References

Angel, R., Matthies, D., and Conrad, R.: Activation of methanogenesis in arid biological soil crusts despite the presence of oxygen, PloS one, 6, e20 453, https://doi.org/10.1371/journal.pone.0020453, 2011.

Armstrong, J. and Armstrong, W.: Light-enhanced convective throughflow increases oxygenation in rhizomes and rhizosphere of Phragmites australis (Cav.) Trin. ex Steud, New Phytologist, 114, 121–128, https://doi.org/10.1111/j.1469-8137.1990.tb00382.x, 1990.

Armstrong, J. and Armstrong, W.: A convective through-flow of gases in Phragmites australis (Cav.) Trin. ex Steud, Aquatic botany, 39, 75–88, https://doi.org/10.1016/0304-3770(91)90023-X, 1991.

Armstrong, J., Armstrong, W., and Beckett, P. M.: Phragmites australis: Venturi- and humidity-induced pressure flows enhance rhizome aeration and rhizosphere oxidation, New Phytologist, 120, 197–207, https://doi.org/10.1111/j.1469-8137.1992.tb05655.x, 1992.

Bade, K., Manz, W., and Szewzyk, U.: Behavior of sulfate reducing bacteria under oligotrophic conditions and oxygen stress in particle-free systems related to drinking water, FEMS Microbiology Ecology, 32, 215–223, https://doi.org/10.1111/j.1574-6941.2000.tb00714.x, 2000.

Barrett, T., Dowle, M., Srinivasan, A., Gorecki, J., Chirico, M., and Hocking, T.: data.table: Extension of 'data.frame'. R package version 1.15.4, https://doi.org/10.32614/CRAN.package.data.table, 2024.

Bastviken, D., Tranvik, L. J., Downing, J. A., Crill, P. M., and Enrich-Prast, A.: Freshwater methane emissions offset the continental carbon sink, Science, 331, 50, https://doi.org/10.1126/science.1196808, 2011.

Baur, P. A.: Multi-year data set of CO_2 fluxes, CH_4 fluxes and environmental parameters of the wetland with reeds at Lake Neusiedl from mid-2018 to 2022. V1. PHAIDRA Repositorium (University of Vienna), https://doi.org/10.25365/phaidra.490, 2024.

Baur, P. A., Henry Pinilla, D., and Glatzel, S.: Is ebullition or diffusion more important as methane emission pathway in a shallow subsaline lake?, Science of the Total Environment, 912, 169 112, https://doi.org/10.1016/j.scitotenv.2023.169112, 2024a.

Baur, P. A., Maier, A., Buchsteiner, C., Zechmeister, T., and Glatzel, S.: Consequences of intense drought on CO_2 and CH_4 fluxes of the reed ecosystem at Lake Neusiedl, Environmental research, 262, 119 907, https://doi.org/10.1016/j.envres.2024.119907, 2024b.

Bokulich, N. A., Kaehler, B. D., Rideout, J. R., Dillon, M., Bolyen, E., Knight, R., Huttley, G. A., and Gregory Caporaso, J.: Optimizing taxonomic classification of marker-gene amplicon sequences with QIIME 2's q2-feature-classifier plugin, Microbiome, 6, 1–17, https://doi.org/10.1186/s40168-018-0470-z, 2018.

Bolyen, E., Rideout, J. R., Dillon, M. R., Bokulich, N. A., Abnet, C. C., Al-Ghalith, G. A., Alexander, H., Alm, E. J., Arumugam, M., Asnicar, F., Bai, Y., Bisanz, J. E., Bittinger, K., Brejnrod, A., Brislawn, C. J., Brown, C. T., Callahan, B. J., Caraballo-Rodríguez, A. M., Chase, J., Cope, E. K., Da Silva, R., Diener, C., Dorrestein, P. C., Douglas, G. M., Durall, D. M., Duvallet, C., Edwardson, C. F., Ernst, M., Estaki, M., Fouquier, J., Gauglitz, J. M., Gibbons, S. M., Gibson, D. L., Gonzalez, A., Gorlick, K., Guo, J., Hillmann, B., Holmes, S., Holste, H., Huttenhower, C., Huttley, G. A., Janssen, S., Jarmusch, A. K., Jiang, L., Kaehler, B. D., Kang, K. B., Keefe, C. R., Keim, P., Kelley, S. T., Knights, D., Koester, I., Kosciolek, T., Kreps, J., Langille, M. G. I., Lee, J., Ley, R., Liu, Y.-X., Loftfield, E., Lozupone, C., Maher, M., Marotz, C., Martin, B. D., McDonald, D., McIver, L. J., Melnik, A. V., Metcalf, J. L., Morgan, S. C., Morton, J. T., Naimey, A. T., Navas-Molina, J. A., Nothias, L. F., Orchanian, S. B., Pearson, T., Peoples, S. L., Petras, D., Preuss, M. L., Pruesse, E., Rasmussen, L. B., Rivers, A., Robeson, M. S., Rosenthal, P., Segata, N., Shaffer, M., Shiffer, A., Sinha, R., Song, S. J., Spear, J. R., Swafford, A. D., Thompson, L. R., Torres, P. J., Trinh, P., Tripathi, A., Turnbaugh, P. J., Ul-Hasan, S., van der Hooft, J. J. J., Vargas, F., Vázquez-Baeza, Y., Vogtmann, E., von Hippel, M., Walters, W., Wan, Y., Wang, M., Warren, J., Weber, K. C., Williamson, C. H. D., Willis, A. D., Xu, Z. Z., Zaneveld, J. R., Zhang, Y., Zhu, Q., Knight, R., and Caporaso, J. G.: Reproducible, interactive, scalable and extensible microbiome data science using QIIME 2, Nature Biotechnology, 37, 852–857, https://doi.org/10.1038/s41587-019-0209-9, 2019.

https://doi.org/10.5194/egusphere-2025-443
Preprint. Discussion started: 6 February 2025
© Author(s) 2025. CC BY 4.0 License.

Bonin, A. S. and Boone, D. R.: The Order Methanobacteriales, in: The Prokaryotes, edited by Dworkin, M., Falkow, S., Rosenberg, E., Schleifer, K., and Stackebrandt, E., pp. 231–243, Springer, New York, NY, https://doi.org/10.1007/0-387-30743-5_11, 2006.

Brix, H.: Gas exchange through dead culms of reed, Phragmites australis (Cav.) Trin. ex Steudel, Aquatic botany, 35, 81–98, https://doi.org/10.1016/0304-3770(89)90069-7, 1989.

Brix, H., Sorrell, B. K., and Schierup, H.-H.: Gas fluxes achieved by in situ convective flow in Phragmites australis, Aquatic botany, 54, 151–163, https://doi.org/10.1016/0304-3770(96)01042-X, 1996.

Brix, H., Sorrell, B. K., and Lorenzen, B.: Are Phragmites-dominated wetlands a net source or net sink of greenhouse gases?, Aquatic botany, 69, 313–324, https://doi.org/10.1016/S0304-3770(01)00145-0, 2001.

Buchsteiner, C., Baur, P. A., and Glatzel, S.: Spatial Analysis of Intra-Annual Reed Ecosystem Dynamics at Lake Neusiedl Using RGB Drone Imagery and Deep Learning, Remote sensing, 15, 3961, https://doi.org/10.3390/rs15163961, 2023.

Caporaso, J. G., Lauber, C. L., Walters, W. A., Berg-Lyons, D., Lozupone, C. A., Turnbaugh, P. J., Fierer, N., and Knight, R.: Global patterns of 16S rRNA diversity at a depth of millions of sequences per sample, Proceedings of the National Academy of Sciences of the United States of America, 108, 4516–4522, https://doi.org/10.1073/pnas.1000080107, 2011.

Castelle, C. J., Méheust, R., Jaffe, A. L., Seitz, K., Gong, X., Baker, B. J., and Banfield, J. F.: Protein Family Content Uncovers Lineage Relationships and Bacterial Pathway Maintenance Mechanisms in DPANN Archaea, Frontiers in Microbiology, 12, 1–13, https://doi.org/10.3389/fmicb.2021.660052, 2021.

Chanton, J. P., Arkebauer, T. J., Harden, H. S., and Verma, S. B.: Diel variation in lacunal CH_4 and CO_2 concentration and $\delta^{13}C$ in Phragmites australis, Biogeochemistry, 59, 287–301, https://doi.org/10.1023/A:1016067610783, 2002.

Conrad, R.: Contribution of hydrogen to methane production and control of hydrogen concentrations in methanogenic soils and sediments, FEMS Microbiology Ecology, 28, 193–202, https://doi.org/10.1016/S0168-6496(98)00086-5, 1999.

Conrad, R.: Microbial Ecology of Methanogens and Methanotrophs, Advances in Agronomy, 96, 1–63, https://doi.org/10.1016/S0065-2113(07)96005-8, 2007.

Conrad, R.: Importance of hydrogenotrophic, aceticlastic and methylotrophic methanogenesis for methane production in terrestrial, aquatic and other anoxic environments: A mini review, Pedosphere, 30, 25–39, https://doi.org/10.1016/S1002-0160(18)60052-9, 2020a.

Conrad, R.: Methane Production in Soil Environments-Anaerobic Biogeochemistry and Microbial Life between Flooding and Desiccation, Microorganisms, 8, https://doi.org/10.3390/microorganisms8060881, 2020b.

Csaplovics, E.: Der Schilfgürtel des Neusiedler Sees, Österreichische Wasser- und Abfallwirtschaft, 71, 494–507, https://doi.org/10.1007/s00506-019-00622-2, 2019.

Duan, X., Wang, X., and Ouyang, Z.: Plant-Mediated CH_4 Emission from a Phragmites-Dominated Wetland in an Arid Region, China, Journal of Freshwater Ecology, 21, 139–145, https://doi.org/10.1080/02705060.2006.9664106, 2006.

Egger, M., Lenstra, W., Jong, D., Meysman, F. J., Sapart, C. J., Van Der Veen, C., Röckmann, T., Gonzalez, S., and Slomp, C. P.: Rapid sediment accumulation results in high methane effluxes from coastal sediments, PLoS ONE, 11, 1–22, https://doi.org/10.1371/journal.pone.0161609, 2016.

Fisher, R. E., France, J. L., Lowry, D., Lanoisellé, M., Brownlow, R., Pyle, J. A., Cain, M., Warwick, N., Skiba, U. M., Drewer, J., Dinsmore, K. J., Leeson, S. R., Bauguitte, S. J.-B., Wellpott, A., O'Shea, S. J., Allen, G., Gallagher, M. W., Pitt, J., Percival, C. J., Bower, K., George, C., Hayman, G. D., Aalto, T., Lohila, A., Aurela, M., Laurila, T., Crill, P. M., McCalley, C. K., and Nisbet, E. G.: Measurement of the ^{13}C isotopic signature of methane emissions from northern European wetlands, Global Biogeochemical Cycles, 31, 605–623, https://doi.org/10.1002/2016GB005504, 2017.

https://doi.org/10.5194/egusphere-2025-443
Preprint. Discussion started: 6 February 2025
© Author(s) 2025. CC BY 4.0 License.

France, J. L., Fisher, R. E., Lowry, D., Allen, G., Andrade, M. F., Bauguitte, S. J.-B., Bower, K., Broderick, T. J., Daly, M. C., Forster, G., Gondwe, M., Helfter, C., Hoyt, A. M., Jones, A. E., Lanoisellé, M., Moreno, I., Nisbet-Jones, P. B. R., Oram, D., Pasternak, D., Pitt, J. R., Skiba, U., Stephens, M., Wilde, S. E., and Nisbet, E. G.: δ^{13}C methane source signatures from tropical wetland and rice field emissions, Philosophical transactions. Series A, Mathematical, physical, and engineering sciences, 380, 20200 449, https://doi.org/10.1098/rsta.2020.0449, 2022.

Friedman, J. and Alm, E. J.: Inferring Correlation Networks from Genomic Survey Data, PLoS Computational Biology, 8, 1–11, https://doi.org/10.1371/journal.pcbi.1002687, 2012.

Galushko, A. and Kuever, J.: Desulfatiglans, in: Bergey's Manual of Systematics of Archaea and Bacteria, pp. 1–4, Wiley, https://doi.org/10.1002/9781118960608.gbm01679, 2019.

Garcia, J.-L., Ollivier, B., and Whitman, W. B.: The Order Methanomicrobiales, in: The Prokaryotes, edited by Dworkin, M., Falkow, S., Rosenberg, E., Schleifer, K., and Stackebrandt, E., pp. 208–230, Springer, New York, NY, https://doi.org/10.1007/0-387-30743-5_10, 2006.

Gardener, W. H.: Chapter 21: Water Content, in: Methods of soil analysis. Part 1, Physical and mineralogical methods, edited by Klute, A., Agronomy, pp. 493–544, Amer. Soc. of Agronomy, Madison, Wisc., ISBN 9780891188643, 1986.

Hammer, U. T.: Saline lake ecosystems of the world, vol. 59 of *Monographiae Biologicae*, Junk, Dordrecht [et al.], ISBN 9061935350, 1986.

Hattori, S.: Syntrophic Acetate-Oxidizing Microbes in Methanogenic Environments, Microbes and Environments, 23, 118–127, https://doi.org/10.1264/jsme2.23.118, 2008.

Hilderbrand, R. H., Keller, S. R., Laperriere, S. M., Santoro, A. E., Cessna, J., and Trott, R.: Microbial communities can predict the ecological condition of headwater streams, PloS one, 15, e0236 932, https://doi.org/10.1371/journal.pone.0236932, 2020.

Hoehler, T. M., Alperin, M. J., Albert, D. B., and Martens, C. S.: Field and laboratory studies of methane oxidation in an anoxic marine sediment: Evidence for a methanogen–sulfate reducer consortium, Global Biogeochemical Cycles, 8, 451–463, https://doi.org/10.1029/94GB01800, 1994.

Hoffmann, M., Schulz-Hanke, M., Garcia Alba, J., Jurisch, N., Hagemann, U., Sachs, T., Sommer, M., and Augustin, J.: A simple calculation algorithm to separate high-resolution CH_4 flux measurements into ebullition- and diffusion-derived components, Atmospheric Measurement Techniques, 10, 109–118, https://doi.org/10.5194/amt-10-109-2017, 2017.

Horne, A. J. and Lessner, D. J.: Assessment of the oxidant tolerance of Methanosarcina acetivorans, FEMS microbiology letters, 343, 13–19, https://doi.org/10.1111/1574-6968.12115, 2013.

Huang, W. C., Liu, Y., Zhang, X., Zhang, C. J., Zou, D., Zheng, S., Xu, W., Luo, Z., Liu, F., and Li, M.: Comparative genomic analysis reveals metabolic flexibility of Woesearchaeota, Nature Communications, 12, 1–14, https://doi.org/10.1038/s41467-021-25565-9, 2021.

Jeffrey, L. C., Maher, D. T., Johnston, S. G., Maguire, K., Steven, A. D. L., and Tait, D. R.: Rhizosphere to the atmosphere: contrasting methane pathways, fluxes, and geochemical drivers across the terrestrial–aquatic wetland boundary, Biogeosciences, 16, 1799–1815, https://doi.org/10.5194/bg-16-1799-2019, 2019.

Jones, J.: Microbes and microbial processes in sediments, Philosophical Transactions of the Royal Society of London. Series A, Mathematical and Physical Sciences, 315, 3–17, https://doi.org/10.1098/rsta.1985.0025, 1985.

Jørgensen, B. B. and Kasten, S.: Sulfur cycling and methane oxidation, in: Marine Geochemistry, edited by Schulz, H. D. and Zabel, M., pp. 271–309, Springer, Berlin, Heidelberg, https://doi.org/10.1007/3-540-32144-6_8, 2006.

Kassambara, A.: ggpubr: 'ggplot2' Based Publication Ready Plots. R package version 0.6.0, https://doi.org/10.32614/CRAN.package.ggpubr, 2023a.

https://doi.org/10.5194/egusphere-2025-443
Preprint. Discussion started: 6 February 2025
© Author(s) 2025. CC BY 4.0 License.

Kassambara, A.: rstatix: Pipe-Friendly Framework for Basic Statistical Tests. R package version 0.7.2, https://doi.org/10.32614/CRAN.package.rstatix, 2023b.

Keeling, C. D.: The concentration and isotopic abundances of atmospheric carbon dioxide in rural areas, Geochimica et cosmochimica acta, 13, 322–334, https://doi.org/10.1016/0016-7037(58)90033-4, 1958.

Kim, J., Verma, S. B., Billesbach, D. P., and Clement, R. J.: Diel variation in methane emission from a midlatitude prairie wetland: Significance of convective throughflow in Phragmites australis, Journal of Geophysical Research, 103, 28 029–28 039, https://doi.org/10.1029/98JD02441, 1998.

King, G. M.: Utilization of hydrogen, acetate, and "noncompetitive"; substrates by methanogenic bacteria in marine sediments, Geomicrobiology Journal, 3, 275–306, https://doi.org/10.1080/01490458409377807, 1984.

Lee, M. J. and Zinder, S. H.: Isolation and Characterization of a Thermophilic Bacterium Which Oxidizes Acetate in Syntrophic Association with a Methanogen and Which Grows Acetogenically on H_2-CO_2, Applied and Environmental Microbiology, 54, 124–129, https://doi.org/10.1128/aem.54.1.124-129.1988, 1988.

Legendre, P.: lmodel2: Model II Regression. R package version 1.7-3, https://doi.org/10.32614/CRAN.package.lmodel2, 2018.

Lovley, D. R. and Goodwin, S.: Hydrogen concentrations as an indicator of the predominant terminal electron-accepting reactions in aquatic sediments, Geochimica et Cosmochimica Acta, 52, 2993–3003, https://doi.org/10.1016/0016-7037(88)90163-9, 1988.

Lovley, D. R., Dwyer, D. F., and Klug, M. J.: Kinetic analysiis of competition between sulfate reducers and methanogens for hydrogen in sediments, Applied and Environmental Microbiology, 43, 1373–1379, https://doi.org/10.1128/aem.43.6.1373-1379.1982, 1982.

Lyu, Z. and Lu, Y.: Metabolic shift at the class level sheds light on adaptation of methanogens to oxidative environments, The ISME Journal, 12, 411–423, https://doi.org/10.1038/ismej.2017.173, 2018.

Martin, M.: Cutadapt removes adapter sequences from high-throughput sequencing reads, EMBnet.journal, 17, 10–12, https://doi.org/10.14806/ej.17.1.200, 2011.

Müller, K.: hms: Pretty Time of Day. R package version 1.1.3, https://doi.org/10.32614/CRAN.package.hms, 2023.

Muyzer, G. and Stams, A. J.: The ecology and biotechnology of sulphate-reducing bacteria, Nature Reviews Microbiology, 6, 441–454, https://doi.org/10.1038/nrmicro1892, 2008.

Pataki, D. E., Ehleringer, J. R., Flanagan, L. B., Yakir, D., Bowling, D. R., Still, C. J., Buchmann, N., Kaplan, J. O., and Berry, J. A.: The application and interpretation of Keeling plots in terrestrial carbon cycle research, Global Biogeochemical Cycles, 17, https://doi.org/10.1029/2001GB001850, 2003.

Philipp, K., Juang, J.-Y., Deventer, M. J., and Klemm, O.: Methane Emissions from a Subtropical Grass Marshland, Northern Taiwan, Wetlands, 37, 1145–1157, https://doi.org/10.1007/s13157-017-0947-8, 2017.

R Core Team: R: A Language and Environment for Statistical Computing, R Foundation for Statistical Computing, Vienna, Austria, https://www.R-project.org/, 2022.

Rosentreter, J. A., Borges, A. V., Deemer, B. R., Holgerson, M. A., Liu, S., Song, C., Melack, J., Raymond, P. A., Duarte, C. M., Allen, G. H., Olefeldt, D., Poulter, B., Battin, T. I., and Eyre, B. D.: Half of global methane emissions come from highly variable aquatic ecosystem sources, Nature Geoscience, 14, 225–230, https://doi.org/10.1038/s41561-021-00715-2, 2021.

Sanders-DeMott, R., Eagle, M. J., Kroeger, K. D., Wang, F., Brooks, T. W., O'Keefe Suttles, J. A., Nick, S. K., Mann, A. G., and Tang, J.: Impoundment increases methane emissions in Phragmites-invaded coastal wetlands, Global Change Biology, 28, 4539–4557, https://doi.org/10.1111/gcb.16217, 2022.

https://doi.org/10.5194/egusphere-2025-443
Preprint. Discussion started: 6 February 2025
© Author(s) 2025. CC BY 4.0 License.

Sass, H., Wieringa, E., Cypionka, H., Babenzien, H. D., and Overmann, J.: High genetic and physiological diversity of sulfate-reducing bacteria isolated from an oligotrophic lake sediment, Archives of Microbiology, 170, 243–251, https://doi.org/10.1007/s002030050639, 1998.

Saunois, M., Stavert, A. R., Poulter, B., Bousquet, P., Canadell, J. G., Jackson, R. B., Raymond, P. A., Dlugokencky, E. J., Houweling, S., Patra, P. K., Ciais, P., Arora, V. K., Bastviken, D., Bergamaschi, P., Blake, D. R., Brailsford, G., Bruhwiler, L., Carlson, K. M., Carrol, M., Castaldi, S., Chandra, N., Crevoisier, C., Crill, P. M., Covey, K., Curry, C. L., Etiope, G., Frankenberg, C., Gedney, N., Hegglin, M. I., Höglund-Isaksson, L., Hugelius, G., Ishizawa, M., Ito, A., Janssens-Maenhout, G., Jensen, K. M., Joos, F., Kleinen, T., Krummel, P. B., Langenfelds, R. L., Laruelle, G. G., Liu, L., Machida, T., Maksyutov, S., McDonald, K. C., McNorton, J., Miller, P. A., Melton, J. R., Morino, I., Müller, J., Murguia-Flores, F., Naik, V., Niwa, Y., Noce, S., O'Doherty, S., Parker, R. J., Peng, C., Peng, S., Peters, G. P., Prigent, C., Prinn, R., Ramonet, M., Regnier, P., Riley, W. J., Rosentreter, J. A., Segers, A., Simpson, I. J., Shi, H., Smith, S. J., Steele, L. P., Thornton, B. F., Tian, H., Tohjima, Y., Tubiello, F. N., Tsuruta, A., Viovy, N., Voulgarakis, A., Weber, T. S., van Weele, M., van der Werf, G. R., Weiss, R. F., Worthy, D., Wunch, D., Yin, Y., Yoshida, Y., Zhang, W., Zhang, Z., Zhao, Y., Zheng, B., Zhu, Q., Zhu, Q., and Zhuang, Q.: The Global Methane Budget 2000–2017, Earth System Science Data, 12, 1561–1623, https://doi.org/10.5194/essd-12-1561-2020, 2020.

Schink, B.: Energetics of syntrophic cooperation in methanogenic degradation, Microbiology and Molecular Biology Reviews, 61, 262–280, https://doi.org/10.1128/mmbr.61.2.262-280.1997, 1997.

Schlesinger, W. H. and Bernhardt, E. S.: Chapter 7 - Wetland Ecosystems, in: Biogeochemistry (Third Edition), edited by Schlesinger, W. H. and Bernhardt, E. S., pp. 233–274, Academic Press, https://doi.org/10.1016/B978-0-12-385874-0.00007-8, 2013.

Sela-Adler, M., Ronen, Z., Herut, B., Antler, G., Vigderovich, H., Eckert, W., and Sivan, O.: Co-existence of methanogenesis and sulfate reduction with common substrates in sulfate-rich estuarine sediments, Frontiers in Microbiology, 8, 1–11, https://doi.org/10.3389/fmicb.2017.00766, 2017.

Shannon, P., Markiel, A., Ozier, O., Baliga, N. S., Wang, J. T., Ramage, D., Amin, N., Schwikowski, B., and Ideker, T.: Cytoscape: A Software Environment for Integrated Models of Biomolecular Interaction Networks, Genome Research, 13, 2498–2504, https://doi.org/10.1101/gr.1239303, 2003.

Soman, V., Suresh, A., Krishnankutty Remani, A., Kalladathvalappil Venugopalan, V., and Keedakkadan, H. R.: A Holistic Review on Diverse Lipid Biomarkers as Environmental Indicators: Extraction and Analysis from Sediments to Microbial Communities, Geomicrobiology Journal, 41, 891–909, https://doi.org/10.1080/01490451.2024.2397685, 2024.

Spormann, A. M. and Thauer, R. K.: Anaerobic acetate oxidation to CO_2 by Desulfotomaculum acetoxidans - Demonstration of enzymes required for the operation of an oxidative acetyl-CoA/carbon monoxide dehydrogenase pathway, Archives of Microbiology, 150, 374–380, https://doi.org/10.1007/BF00408310, 1988.

Sriskantharajah, S., Fisher, R. E., Lowry, D., Aalto, T., Hatakka, J., Aurela, M., LAURILA, T., Lohila, A., Kuitunen, E., and Nisbet, E. G.: Stable carbon isotope signatures of methane from a Finnish subarctic wetland, Tellus B: Chemical and Physical Meteorology, 64, 18 818, https://doi.org/10.3402/tellusb.v64i0.18818, 2012.

Stams, A. J. M., Teusink, B., and Sousa, D. Z.: Ecophysiology of Acetoclastic Methanogens, in: Biogenesis of Hydrocarbons. Handbook of Hydrocarbon and Lipid Microbiology, edited by Stams, A. J. M. and Sousa, D. Z., pp. 1–14, Springer, Cham, https://doi.org/10.1007/978-3-319-53114-4_21-1, 2019.

Valentine, D. L.: Biogeochemistry and microbial ecology of methane oxidation in anoxic environments: a review, Antonie van Leeuwenhoek, 81, 271–282, https://doi.org/10.1023/A:1020587206351, 2002.

https://doi.org/10.5194/egusphere-2025-443
Preprint. Discussion started: 6 February 2025
© Author(s) 2025. CC BY 4.0 License.

Valentine, D. L. and Reeburgh, W. S.: New perspectives on anaerobic methane oxidation, Environmental Microbiology, 2, 477–484, https://doi.org/10.1046/j.1462-2920.2000.00135.x, 2000.

van den Berg, M., Ingwersen, J., Lamers, M., and Streck, T.: The role of Phragmites in the CH_4 and CO_2 fluxes in a minerotrophic peatland in southwest Germany, Biogeosciences, 13, 6107–6119, https://doi.org/10.5194/bg-13-6107-2016, 2016.

van den Berg, M., van den Elzen, E., Ingwersen, J., Kosten, S., Lamers, L. P. M., and Streck, T.: Contribution of plant-induced pressurized flow to CH_4 emission from a Phragmites fen, Scientific reports, 10, https://doi.org/10.1038/s41598-020-69034-7, 2020.

Vroom, R., van den Berg, M., Pangala, S. R., van der Scheer, O. E., and Sorrell, B. K.: Physiological processes affecting methane transport by wetland vegetation – A review, Aquatic Botany, 182, 103 547, https://doi.org/10.1016/j.aquabot.2022.103547, 2022.

Wang, Z., Zeng, D., and Patrick, W. H.: Methane emissions from natural wetlands, Environmental monitoring and assessment, 42, 143–161, https://doi.org/10.1007/BF00394047, 1996.

Whiticar, M., Faber, E., and Schoell, M.: Biogenic methane formation in marine and freshwater environments: CO_2 reduction vs. acetate fermentation—Isotope evidence, Geochimica et cosmochimica acta, 50, 693–709, https://doi.org/10.1016/0016-7037(86)90346-7, 1986.

Whiticar, M. J.: Carbon and hydrogen isotope systematics of bacterial formation and oxidation of methane, Chemical Geology, 161, 291–314, https://doi.org/10.1016/S0009-2541(99)00092-3, 1999.

Whitman, W. B. and Jeanthon, C.: Methanococcales, in: The Prokaryotes, edited by Dworkin, M., Falkow, S., Rosenberg, E., Schleifer, K.-H., and Stackebrandt, E., pp. 257–273, Springer, New York, NY, https://doi.org/10.1007/0-387-30743-5_13, 2006.

Wickham, H.: ggplot2: Elegant Graphics for Data Analysis, Springer-Verlag New York, ISBN 978-3-319-24277-4, https://ggplot2.tidyverse.org, 2016.

Wickham, H., Pedersen, T. L., and Seidel, D.: scales: Scale Functions for Visualization. R package version 1.3.0, https://doi.org/10.32614/CRAN.package.scales, 2023.

Wolfram, G. and Herzig, A.: Nährstoffbilanz Neusiedler See, Wiener Mitteilungen, 228, 317–338, https://www.dws-hydro-oekologie.at/wp-content/uploads/wolfram_herzig_2013.pdf, 2013.

Wörner, S. and Pester, M.: The active sulfate-reducing microbial community in littoral sediment of oligotrophic lake constance, Frontiers in Microbiology, 10, 247, https://doi.org/10.3389/fmicb.2019.00247, 2019.

Zhang, B., Li, Y., Xiang, S.-Z., Yan, Y., Yang, R., Lin, M.-P., Wang, X.-M., Xue, Y.-L., and Guan, X.-Y.: Sediment Microbial Communities and Their Potential Role as Environmental Pollution Indicators in Xuande Atoll, South China Sea, Frontiers in microbiology, 11, 1011, https://doi.org/10.3389/fmicb.2020.01011, 2020.

Zhang, Q., Sun, R., Jiang, G., Xu, Z., and Liu, S.: Carbon and energy flux from a Phragmites australis wetland in Zhangye oasis-desert area, China, Agricultural and Forest Meteorology, 230-231, 45–57, https://doi.org/10.1016/j.agrformet.2016.02.019, 2016.